Research Square

Preprints are preliminary reports that have not undergone peer review.
They should not be considered conclusive, used to inform clinical practice,
or referenced by the media as validated information.

Phenotype-genotype spectrum in CTNND2-related neurodevelopmental disease

Mansoureh Shahsavani
Karolinska Institutet
Josephine Wincent
Karolinska Institutet
Ricarda Reiter
Johannes Kepler University of Linz
Andrea Soltysova
Comenius University Bratislava
Jakob Schuy
Karolinska Institutet
Hafdis T. Helgadottir
Karolinska Institutet
Jesper Eisfeldt
Karolinska University Hospital
Marlene Ek
Karolinska Institutet
Andrej Ficek
Comenius University Bratislava
Lotta Druschke
Karolinska Institutet
Katarina Kusikova
Comenius University and National Institute of Children´s Diseases
Tzung-Chien Hsieh
University Hospital Bonn
Aron Kirchhoff
University Hospital Bonn
Peter Krawitz
University Hospital Bonn
Jing-Mei Li
University Hospital Bonn
Gerald Webersinke
Ordensklinikum Linz Barmherzige Schwestern
Svetlana Gorokhova

Centre de Génétique Médicale de Marseille
Chantal Missirian
Centre de Génétique Médicale de Marseille
Florence Riccardi
Aix-Marseille Université
Lisa Pavinato
University of Turin
Alfredo Brusco
University of Turin
Giorgia Mandrile
University of Turin
Slavica Trajkova
University of Turin
Francesco Pintus
University of Turin
Biljana Gagachovska
Ss. Cyril and Methodius University in Skopje
Quinten Waisfisz
Amsterdam University Medical Centers
Johanna M van Hagen
Amsterdam University Medical Centers
Emma Bedoukian
Children's Hospital of Philadelphia
Kosuke Izumi
Children's Hospital of Philadelphia
Leslie Granger
University Medical Center Utrecht
Andrea Petersen
University Medical Center Utrecht
Renske Oegema
University Medical Center Utrecht
Manon Huibers
University Medical Center Utrecht
Florence Demurger
Centre hospitalier Bretagne Atlantique
Elise Brischoux-Boucher
Université Marie et Louis Pasteur
Sophie Julia
Centre Hospitalier Universitaire de Toulouse

Guillaume Banneau
Centre Hospitalier Universitaire de Toulouse
M Jesus Zavala
Universidad del Desarrollo
Catalina Lagos
Universidad del Desarrollo
Gabriela M Repetto
Universidad del Desarrollo
Guillaume Jouret
Laboratoire National de Santé
Catherine Kentros
Columbia University
Mythily Ganapathi
Columbia University Irving Medical Center
Wendy K. Chung
Boston Children's Hospital
Halie May
Columbia University Irving Medical Center
Susan M. Hiatt
HudsonAlpha Institute for Biotechnology
Whitley V. Kelley
HudsonAlpha Institute for Biotechnology
Alisa Förster
Medizinische Hochschule Hannover
Lisa Olfe
Medizinische Hochschule Hannover
Amelle Shillington
University of Cincinnati
Benjamin Dauriat
Centre Hospitalier Universitaire de Limoges
Sandra Mercier
Centre Hospitalier Universitaire de Nantes
Benjamin Cogné
Centre Hospitalier Universitaire de Nantes
Camille Engel
Centre Hospitalier Universitaire de Besançon
Eric Dahlen
Centre Hospitalier Universitaire de Besançon
Georg Rosenberger

University Medical Center Hamburg-Eppendorf
Thomas Sauvigny
University Medical Center Hamburg-Eppendorf
Hamza Hadj Abdallah
Hôpital Necker-Enfants Malades
Thomas Courtin
Hôpital Necker-Enfants Malades
Asbjørg Stray-Pedersen
Oslo University Hospital
John A. Bernat
University of Iowa Health Care
Vitoria K Paolillo
Children's Mercy Hospital
Florencia Del Viso
Children's Mercy Hospital
Joseph T Alaimo
Children's Mercy Hospital
Isabelle Thiffault
Children's Mercy Hospital
Emily G Farrow
Children's Mercy Hospital
Ana S.A. Cohen
Children's Mercy Hospital
Serge Weis
Kepler Universitätsklinikum
Hans-Christoph Duba
Johannes Kepler University of Linz
Ann Nordgren
Karolinska Institutet
Anna Falk
Karolinska Institutet
Denisa Weis
Johannes Kepler University of Linz
Anna Lindstrand
anna.lindstrand@ki.se

Karolinska Institutet

Research Article

Keywords: CTNND2, intellectual disability, haploinsufficiency, neurodevelopmental disorder, early neurogenesis, δ-catenin, induced pluripotent stem cells, WNT signaling, CRISPR-Cas9

Posted Date: November 12th, 2026

DOI: https://doi.org/10.21203/rs.3.rs-11483188/v1

License: This work is licensed under a Creative Commons Attribution 4.0 International License.
Read Full License

Additional Declarations: No competing interests reported.

Phenotype-genotype spectrum in *CTNND2*-related neurodevelopmental disease

Mansoureh Shahsavani[1,2 # §], Josephine Wincent[1,2 # §], Ricarda Reiter[3], Andrea Soltysova[4,5], Jakob Schuy[1], Hafdis T. Helgadottir[1,2], Jesper Eisfeldt[1,2,6], Marlene Ek[1,2], Andrej Ficek[4], Lotta Druschke[1], Katarina Kusikova[7], Tzung-Chien Hsieh[8], Aron Kirchhoff[8], Peter Krawitz[8], Jing-Mei Li[8], Gerald Webersinke[9], Svetlana Gorokhova[10,11], Chantal Missirian[10,11], Florence Riccardi[11,12], Lisa Pavinato[13], Alfredo Brusco[13,14], Giorgia Mandrile[15], Slavica Trajkova[13], Francesco Pintus[16], Biljana Gagachovska[17], Quinten Waisfisz[18], Johanna M van Hagen[18], Emma Bedoukian[19], Kosuke Izumi[19], Leslie Granger[20], Andrea Petersen[20], Renske Oegema[20], Manon Huibers[20], Florence Demurger[21], Elise Brischoux-Boucher[22], Sophie Julia[23], Guillaume Banneau[23], M Jesus Zavala[24], Catalina Lagos[25], Gabriela M Repetto[25], Guillaume Jouret[26], Catherine Kentros[27], Mythily Ganapathi[28], Wendy K. Chung[29], Halie May[30], Susan M. Hiatt[31], Whitley V. Kelley[31], Alisa Förster[32], Lisa Olfe[32], Amelle Shillington[33,34], Benjamin Dauriat[35], Sandra Mercier[36], Benjamin Cogné[36], Camille Engel[37], Eric Dahlen[38], Georg Rosenberger[39], Thomas Sauvigny[40], Hamza Hadj Abdallah[41], Thomas Courtin[41], Asbjørg Stray-Pedersen[42], John A. Bernat[43], Vitoria K Paolillo [44], Florencia Del Viso [44], Joseph T Alaimo [44,45], Isabelle Thiffault [44,45], Emily G Farrow [44,45], Ana S.A. Cohen [44,45], Serge Weis [46,47], Hans-Christoph Duba[3], Ann Nordgren[1,2,48,49], Anna Falk[50,51], Denisa Weis[3#*], Anna Lindstrand[1,2,6#*]

[1]Department of Molecular Medicine and Surgery, Karolinska Institutet, Stockholm, Sweden
[2]Department of Clinical Genetics and Genomics, Karolinska University Hospital, Stockholm, Sweden
[3]Institute of Medical Genetics, Med Campus IV, Johannes Kepler University Linz, Linz, Austria
[4]Department of Molecular Biology, Faculty of Natural Science, Comenius University, Bratislava, Slovakia
[5]Institute for Clinical and Translational Research, Biomedical Research Centre, Slovak Academy of Sciences, Bratislava, Slovakia
[6]Science for Life Laboratory, Department of Molecular Medicine and Surgery, Karolinska Institutet, Stockholm, Sweden
[7]Department of Pediatric Neurology, Faculty of Medicine, Comenius University and National Institute of Children´s Diseases, Bratislava, Slovakia
[8]Institute for Genomic Statistics and Bioinformatics, University Hospital Bonn, Rheinische Friedrich-Wilhelms-Universität Bonn, Bonn, Germany
[9]Laboratory for Molecular Genetic Diagnostic, Ordensklinikum Linz Barmherzige Schwestern, Linz, Austria
[10]Department of Medical Genetics, La Timone Children Hospital, AP-HM, Marseille, France
[11] Aix Marseille Univ, INSERM, MMG, U 1251, Marseille, France
[12] Medical genetics department, Sainte Musse Hospital, CHITS, Toulon, France
[13]Department of Neurosciences, Rita Levi-Montalcini, University of Torino, 10126 Turin, Italy
[14] Città della Salute e della Scienza University Hospital, Medical Genetics unit, 10126, Turin, Italy
[15]Medical Genetics Unit and Thalassemia Center, San Luigi University Hospital, University of Torino, Orbassano, Italy
[16]Department of Clinical and Biological Sciences, University of Turin, Orbassano, Italy.
[17] Department of Child and Adolescent Psychiatry, University Clinic of Psychiatry, Faculty of Medicine, Ss. Cyril and Methodius University, Skopje, Republic of North Macedonia
[18]Department of Human Genetics, Amsterdam UMC, Amsterdam, The Netherlands
[19]Childrens Hospital of Philadelphia, Philadelphia, PA, USA
[20]Department of Genetics, Division of Laboratories, Pharmacy and Biomedical Genetics, Utrecht University, University Medical Center Utrecht, Utrecht, the Netherlands
[21]Service de Génétique, CHBA, Vannes, France
[22]Centre de génétique humaine, CHU Besançon, Université Marie et Louis Pasteur, Besançon, France
[23]Service de Génétique Médicale, CHU Purpan, Toulouse, France

[24]Hospital Base de Valdivia and Rare Diseases Program, Universidad del Desarrollo, Valdivia, Chile
[25]Rare Diseases Program, Instituto de Ciencias e Innovacion en Medicina, Facultad de Medicina Clinica Alemana Universidad del Desarrollo, Santiago, Chile
[26]National Center of Genetics, Clinica Genetics Unit, Laboratoire national de Santé, 1 Rue Louis Rech, Dudelange, Luxembourg
[27]SNF Center for Precision Psychiatry & Mental Health, Columbia University, New York, NY, USA
[28]Department of Pathology & Cell Biology, Columbia University Irving Medical Center, New York, NY, USA
[29]Boston Children's Hospital, Harvard Medical School, Boston, MA, USA
[30]Institute for Genomic Medicine, Columbia University Irving Medical Center, New York, NY, USA
[31]HudsonAlpha Institute for Biotechnology, Huntsville, AL, USA
[32]Department of Human Genetics, Hannover Medical School, Hannover, Germany
[33]Department of Pediatrics, University of Cincinnati College of Medicine, Cincinnati, OH, USA
[34]Division of Human Genetics, Cincinnati Children's Hospital Medical Center, Cincinnati, OH, USA
[35]Service de Cytogénétique et Génétique médicale – Hopital Mère-Enfant, CHU de Limoges, Limoges, France
[36]CHU Nantes, Service de génétique médicale, Nantes, France
[37]Centre de génétique humaine, CHU Besançon, Université de Bourgogne Franche-Comté, Besançon, France
[38]CHU Besançon, Oncobiologie Génétique Bioinformatique, Besançon, France
[39]Institute of Human Genetics, University Medical Center Hamburg-Eppendorf, Hamburg, Germany
[40]Department of Neurosurgery, University Medical Center Hamburg-Eppendorf, Hamburg, Germany
[41]Service de Médecine Génomique des Maladies Rares, Hôpital Necker-Enfants Malades, Paris, France
[42]Norwegian National Unit for Newborn Screening, Division of Paediatric and Adolescent Medicine, Oslo University Hospital, Oslo, Norway
[43]Division of Medical Genetics and Genomics, Stead Family Department of Pediatrics, University of Iowa Health Care, Iowa City, IA, USA
[44]Department of Pathology and Laboratory Medicine, Children's Mercy Kansas City, Kansas City, MO, USA
[45]University of Missouri-Kansas City School of Medicine, Kansas City, MO, USA
[46]Division of Neuropathology, Department of Pathology and Molecular Pathology, Neuromed Campus, Kepler University Hospital, Linz, Austria
[47]Clinical Research Institute for Neurosciences, Johannes Kepler University, Linz, Austria
[48]Department of Laboratory Medicine, Institute of Biomedicine, University of Gothenburg, Gothenburg, Sweden
[49]Department of Clinical Genetics and Genomics, Sahlgrenska University Hospital, Region Västra Götaland, Got henburg, Sweden
[50]Department of Neuroscience, Karolinska Institutet, Stockholm, Sweden
[51]Lund Stem Cell Center, Department of Experimental Medical Science, Science for Life Laboratory, Lund University, Lund, Sweden

§shared first authors

#Equal contribution

*Corresponding authors, Denisa.Weis@kepleruniklinikum.at and anna.lindstrand@ki.se

Abstract

Background: Heterozygous variants in *CTNND2*, encoding the brain-specific protein δ-catenin, are associated with a broad spectrum of neurodevelopmental disorders, including dyslexia, attention deficit hyperactivity disorder, intellectual disability, and autism. Despite its clinical significance, the full phenotypic spectrum of *CTNND2*-associated disorders and the neurodevelopmental role of δ-catenin, a key component of the cadherin-catenin cell adhesion complex, remain poorly defined.

Methods: Through international collaboration, we assembled the phenotypic and molecular information for 57 individuals, 42 previously unpublished, carrying heterozygous *CTNND2* variants. All individuals were evaluated by local clinicians, and the variants were identified through exome or genome sequencing, clinical microarray, or karyotyping. To investigate the effects of δ-catenin loss on early neurogenesis, we performed neural induction and transcriptomic profiling in three patient-derived neuroepithelial stem cell (NESC) lines and three isogenic CRISPR-Cas9-edited *CTNND2* knockout lines. Transcriptomic changes were assessed across the patient-derived and CRISPR-edited models to identify shared and distinct transcriptional alterations, with particular focus on genes within the CTNND2 interactome and WNT- and cadherin-associated networks.

Results: We identified 41 distinct *CTNND2* variants, including 28 novel variants comprising 18 predicted loss-of-function and 10 protein-altering variants. Among cases with parental testing, eight variants occurred de novo and 12 were inherited from an affected parent. The most common clinical features were developmental delay (90%), intellectual disability (74%), and behavioral abnormalities (79%). Neural induction revealed delayed neural rosette formation in one of the three patient-derived lines, whereas the remaining patient-derived and

knockout lines showed apparently normal neural induction. Transcriptomic profiling revealed variable but partly convergent alterations across the patient-derived and knockout models, involving the CTNND2 interactome and WNT and cadherin signaling networks at both developmental time points.

Conclusions: This study defines *CTNND2*-related neurodevelopmental disorders as a clinically recognizable but highly variable phenotype overlapping with other intellectual disability and autism spectrum disorders. Across cellular models, transcriptomic analysis identified variable and partly convergent changes involving interconnected networks associated with CTNND2, WNT, and cadherin signaling. The variability observed across both individuals and cellular models further highlights the influence of genetic background and other modifying factors on the consequences of *CTNND2* disruption. These findings expand the clinical and molecular spectrum of *CTNND2*-associated disorders and provide a framework for further investigation of the molecular consequences of *CTNND2* disruption during early human neural development.
Keywords: *CTNND2*, intellectual disability, haploinsufficiency, neurodevelopmental disorder, early neurogenesis, δ-catenin, induced pluripotent stem cells, WNT signaling, CRISPR-Cas9

BACKGROUND

Loss of function (LoF) variants affecting *CTNND2*, located on the short arm of chromosome 5, have been linked to various neurodevelopmental disorders (NDD) and psychiatric conditions such as intellectual disability (ID) with or without dyslexia-like learning difficulties (Belcaro et al., 2015; Hofmeister et al., 2015), autism spectrum disorder (ASD) (Miller et al., 2020; Turner et al., 2015), attention deficit hyperactivity disorder (ADHD) (Adegbola et al., 2020), and schizophrenia (Chen et al., 2023). Furthermore, a recent report details a consanguineous family in which three siblings carried homozygous deletions at 5p15.2 encompassing 19 of the 22 exons of *CTNND2.* These individuals showed more severe NDD than their heterozygous relatives, providing evidence for a more severe phenotype associated with biallelic *CTNND2* loss of function (Pauly et al., 2024).

CTNND2 encodes δ-catenin, a cytosolic protein belonging to the catenin superfamily. It is part of the cadherin-catenin cell adhesion complex and has been implicated in the canonical WNT/LEF-1-mediated pathway regulating target gene transcription (H. Kim et al., 2012; Zhang et al., 2025). Previous studies in mice have shown that absence of CTNND2 results in severe learning deficits, synaptic plasticity impairments, and alterations in synaptic composition (Israely et al., 2004) as well as dendritic architecture and function (Arikkath et al., 2008, 2009; Kim et al., 2008a, 2008b; K. Kim et al., 2002; Matter et al., 2009). Elevating *Ctnnd2* expression in mice resulted in heightened sociability and decreased anxiety, while homozygous *Ctnnd2* knockout mice exhibited spatial learning deficits and aberrant fear conditioning (Ryu et al., 2019). More recently, using knockdown and knockout zebrafish models for *CTNND2,* we showed abnormal neuron migration and altered gene expression in the forebrain as well as increased swimming activity in both larval and adult stages (Hofmeister et al., 2015; Vaz et al., 2023).

Despite these findings, the phenotypic spectrum associated with heterozygous *CTNND2*

variants and the molecular consequences of *CTNND2* disruption during early human neural development remain incompletely understood. Here, we characterize the clinical spectrum of *CTNND2*-related neurodevelopmental disease using phenotype and genotype data from 57 individuals (including 15 previously published) carrying heterozygous *CTNND2* variants, collected through an international collaboration. We further investigate the effect of *CTNND2* disruption on early neural development using induced pluripotent stem cell-derived neural cells from three affected individuals and three isogenic CRISPR-Cas9-edited *CTNND2* lines. By integrating transcriptomic analyses across patient-derived and isogenic models, we assess shared and variable consequences of *CTNND2* disruption, with particular focus on the CTNND2 interactome and WNT- and cadherin-associated transcriptional networks.

METHODS

Participants

We collected genotype and phenotype information for 57 individuals with heterozygous variants in *CTNND2* (Additional File 1: Table S1). Fifteen individuals had been previously reported (Sanders et al., 2011; Asadollahi et al., 2014; Belcaro et al., 2015; Hofmeister et al., 2015; Adegbola et al., 2020; Pauly et al., 2024; Ambrose et al., 2025). The previously unreported individuals (n=42) were identified through GeneMatcher (http://genematcher.org/) (Sobreira et al., 2015). Clinical information, including developmental history, cognition, neurological manifestations, behavioral features and dysmorphology, was reviewed by local clinicians. Frequencies of clinical features were calculated as the number of affected individuals divided by the number of individuals assessed for each feature. Variants in *CTNND2* classified as pathogenic or likely pathogenic (ACMG classes 5 and 4), as well as missense variants with a REVEL score > 0.4 (Ioannidis et al., 2016) and a gnomAD v2.1.1 allele frequency < 0.000009, were included. The REVEL threshold of >0.4 was chosen as a permissive cutoff to capture

potentially deleterious missense variants, because interpretation of *CTNND2* variants is challenging and pathogenic missense variants may not always reach high prediction scores. Stricter cutoffs (e.g., REVEL >0.7) give higher confidence but may exclude relevant variants. The allele frequency threshold was chosen to include only ultra-rare variants, since pathogenic variants in a rare and highly penetrant neurodevelopmental disorder are not expected to occur at appreciable frequency in population databases.

GestaltMatcher facial analysis

Facial photos from 15 individuals with *CTNND2* variants (N_7-12, N_17, N_17a, N_19, N_23, N_25, N_26, N_32, N_43, and N_58) were analyzed using the GestaltMatcher framework (Hsieh et al., 2022; Mak et al., 2025). Facial similarity was quantified by averaging pairwise cosine distances across 12 embeddings per image, generated using an ensemble model with test-time augmentation (Hustinx et al., 2023). Intra-cohort similarity was assessed by comparing their mean pairwise distance within the CTNND2 group to reference distributions from the GestaltMatcher Database (Lesmann et al., 2024), which includes known syndromes and randomly sampled cohorts. Pairwise comparisons were also performed to evaluate facial similarity at the individual level. An average CTNND2 facial image was created as a composite photo of all 15 individuals. Clinical feature prevalence is summarized in Additional File 1: Table S1, and detailed methods are provided in the supplementary files (Additional File 2: Supplementary methods). The photographs analysed are shown in Additional File 3: Fig. S1C.

Identification and evaluation of genetic variants

CTNND2 variants were identified through karyotyping, clinical microarray analysis, or exome and genome sequencing performed in diagnostic or research settings. Segregation analysis was performed when possible (n = 20). All identified variants were classified according to the

American College of Medical Genetics and Genomics (ACMG) guidelines (Richards et al., 2015) (Additional File 1: Table S1). The Genome Aggregation Database (gnomAD v.2.1.1; https://gnomad.broadinstitute.org/) was used to assess the presence of these variants in control populations. Variant coordinates are based on the *CTNND2* transcript NM_001332.4 and the GRCh37/hg19 reference genome.

Generation of iPSC, NESC, and knockout lines

Skin biopsies were obtained from three healthy controls (C#1, C#2, and C#3) and three individuals with pathogenic *CTNND2* variants. These included a 28-year-old female (N_48 hereafter called P#1) and her mother (N_49 - P#2), both carriers of a balanced chromosomal translocation disrupting *CTNND2*, and a four-year-old male (N_7 - P#3) with a 143 kb heterozygous deletion spanning exons 4-9 of *CTNND2*. Fibroblasts were cultured according to standard protocols and induced pluripotent stem cell (iPSC) lines were generated at the Karolinska Institutet iPS Core facility (Karolinska Institutet, Stockholm, Sweden) as previously described (Kele et al., 2016). Details of all cell lines used are provided in Additional File 1: Table S2.

To assess genomic integrity, the patient-derived iPSC lines were analysed by SNP-array (Illumina Infinium Global Screening Array-24 BeadChip) and optical genome mapping (OGM) (Bionano Saphyr), and the P#1 line also by standard G-banding karyotyping. Details are provided in Additional File 2, and the SNP-array results are summarized in Additional File 1: Table S3). The known *CTNND2*-disrupting translocation in P#1 and P#2 was also confirmed by breakpoint junction PCR (data not shown).

CTNND2 knockout (KO) lines were generated with CRISPR/Cas9 technology and validated at the Karolinska Genome Engineering (KGE) core and the KI iPSCore facilities utilizing C#1 as the parental line. Three clones were selected, characterized, and used for the study: one

heterozygous (KO#1) and two homozygous lines (KO#2 and KO#3; Additional File 3: Fig. S2A). Neuroepithelial stem cells (NESCs) were derived from the nine iPSC lines (Additional File 1: Table S2) as previously described (Calvo-Garrido et al., 2021). Detailed protocols are provided in the supplementary files (Additional File 2: Supplementary methods).

Immunofluorescence staining

Immunofluorescence staining was performed as described in Additional File 2 (Supplementary Methods). Antibodies are listed in Additional File 1: Table S4. For CTNND2 quantification, multiple nonoverlapping confocal images were acquired at 20x magnification using a Zeiss LSM 700 confocal microscope. For each cell line, 3–5 differentiation replicates were analyzed, with nine sections quantified per replicate. Mean CTNND2 fluorescence intensity was measured for each section using ImageJ/Fiji, and the mean fluorescence intensity was calculated for each replicate. Statistical analysis was performed using a two-sided unpaired t-test with Bonferroni correction for multiple comparisons.

Transcriptome analysis

Total RNA was extracted in triplicate at P0 (day 12) and P6 using the RNeasy Mini Kit on the QIAcube Connect robot (QIAGEN). Bulk RNA-Seq was performed using the Illumina TruSeq Stranded mRNA library preparation protocol on a NovaSeq6000 platform (National Genomics Infrastructure, SciLifeLab, Stockholm). Raw sequencing reads were processed using nf-core/rnaseq (Ewels et al., 2020)(github.com/nf-core/rnaseq), including quality control and data cleaning. Reads were aligned to the GRCh38 reference genome using STAR (Dobin et al., 2013) and transcripts were quantified using Salmon (Patro et al., 2017).

Differential gene expression analysis was performed using DeSeq2 (Love et al., 2014), applying a false discovery rate (FDR) threshold of 1% and a 25%-fold-change cutoff. Principal

component analysis (PCA) was used to assess sample clustering. CTNND2 interactors were found using STRING (Szklarczyk et al., 2023). Pathway enrichment was performed using the PANTHER database (Mi et al., 2005), WNT and cadherin pathway genes were annotated based on KEGG pathways (Kanehisa et al., 2016).

RESULTS

Cohort characteristics

We report 42 novel individuals from 29 pedigrees carrying heterozygous variants in *CTNND2*. The novel cohort includes 28 males and 14 females, with a mean age of 15 years (range: 1 day to 49 years). Combined with 15 previously published cases, the total cohort includes 57 individuals: 32 males, 23 females and 2 with unknown sex. The cohort spans both pediatric cases (70%) and adults (21%), with age information unavailable for 9% of individuals. Clinical features were assessed based on the available information for each individual, and the number of assessed individuals therefore varied across phenotypic features. Clinical symptoms at the cohort level are summarized in Table 1, with frequencies calculated based on the number of individuals assessed for each feature. The detailed clinical manifestations are listed in Additional File 1: Table S1.

Table 1: Summary of clinical features of *CTNND2*-related neurodevelopmental disorder.

Phenotypic manifestation	HPO	LoF n=41, 72 %		Protein-altering n=16, 28%		Total n= 57	
Intellectual, social and behavioral development							
Developmental Delay	0001263	25/28	89%	12/13	92%	37/41	90%
Delayed speech and language development	0000750	17/28	61%	12/14	86%	29/42	69%
Intellectual disability (including borderline ID)	0001249	19/26	73%	10/13	77%	29/39	74%
Intellectual disability, borderline	0006889	9/26	35%	1/13	8%	10/39	26%
Intellectual disability, mild	0001256	8/26	31%	2/13	15%	10/39	26%
Intellectual disability, moderate	0002342	0/26	0%	4/13	31%	4/39	10%
Intellectual disability, severe	0010864	0/26	0%	1/13	8%	1/39	3%
Autism	0000717	10/28	36%	4/13	31%	14/41	34%
Atypical behavior	0000708	20/23	87%	7/11	64%	27/34	79%
Aggressive behavior	0000718	6/23	26%	1/11	9%	7/34	21%
Abnormal emotional behavior	0100851	4/23	17%	2/11	18%	6/34	18%
Abnormal social behavior	0012433	2/23	9%	2/11	18%	4/34	11%
ADHD/ADD	0000736/0007018	14/24	58%	1/12	8%	15/36	42%
Epilepsy	0001250	4/25	16%	1/15	7%	5/40	13%
EEG abnormality	0002353	5/8	63%	1/4	25%	6/12	50%
Brain imaging abnormality	0410263	4/14	29%	3/7	43%	7/21	33%
Facial dysmorphism and body abnormalities	0001999	20/32	63%	10/13	77%	30/45	67%
Abnormal shape, size, or slanting of palpebral fissure	0200005, 0200006,0200007	12/29	41%	2/12	17%	14/41	34%
Hyperextensible joint	0001282	5/23	22%	1/16	6%	6/39	15%
Myopia	0000545	8/33	24%	1/13	8%	9/46	20%

HPO: Human Phenotype Ontology; LoF: Loss of Function; ADHD: Attention-Deficit/Hyperactivity Disorder; ADD: Attention-Deficit Disorder.

CTNND2 genotype spectrum

In the 42 novel individuals, we identified 28 distinct *CTNND2* variants, classified as either LoF (n=18, 6 large deletions, 5 nonsense variants and 7 frameshift variants) or protein-altering variants (n=10, 9 missense and one in-frame deletion of one amino acid). One variant, c.2653C>T (p.Arg885*) was identified in two unrelated cases. Among the 20 index cases where parental testing was performed, eight variants were *de novo*, and twelve were inherited from an affected parent. One frameshift variant, c.121del, p.(Asp41Metfs*25), in individual N_13, was mosaic in both peripheral blood (27%) and saliva (variant fraction not quantified).

According to the ACMG criteria, 22 variants were classified as pathogenic or likely pathogenic (LoF variants and four protein-altering variants), while six protein-altering variants were classified as variants of uncertain significance (VUS). Combining our data with previously published cases, this report includes 41 heterozygous *CTNND2* variants in 40 unrelated cases. Of these, 30 were predicted null variants, including 16 large deletions, two translocations, five nonsense variants, and seven frameshift variants. In addition, 16 individuals harbor heterozygous protein-altering variants, including six variants classified as VUS (Fig. 1A, Additional File 1: Table S1).

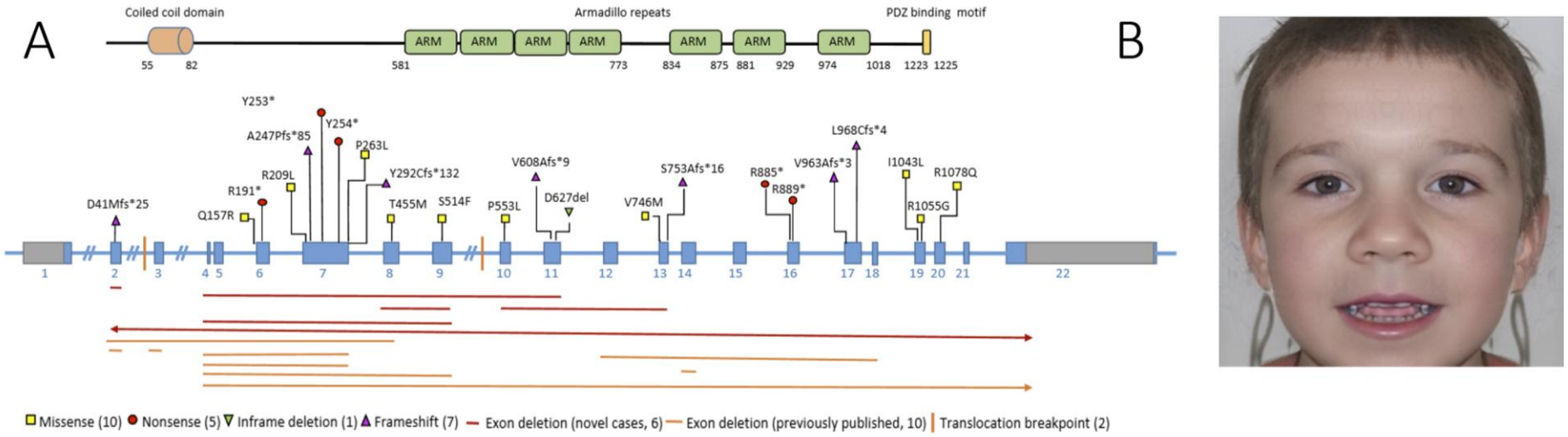


Figure 1. *CTNND2* variant spectrum and facial features. A. Schematic representation of δ-catenin (top) and the *CTNND2* gene (bottom). Genetic variants are indicated at their respective positions on the gene: yellow squares represent missense variants, red circles nonsense variants, a green triangle represents an in-frame deletion, and a purple triangle represents a frameshift variant. Translocation breakpoints are shown as yellow vertical lines. Exon deletions are depicted as horizontal lines in red (new cases) and orange (previously published cases). **B.** Composite facial image of individuals with *CTNND2*-related disorders generated using the GestaltMatcher photorealistic synthetic portrait approach (Kirchhoff et al., 2025).

Frequency of *CTNND2*-associated clinical manifestations

Intellectual- and speech development

Motor developmental delay was reported in 37 of 41 individuals (90%) and delayed speech and language development in 29 of 42 (69%). The mean age for independent sitting was 10.5 months (median 11.5) months; range 6-17 months), and for walking 19 months (median 18; range 9-36 months). The mean age for first spoken words was 19 months (median 22; range 8-60 months). Expressive speech difficulties, including apraxia, delayed speech, and limited sentence formation with the use of simple sentences, were observed in 56% of individuals (13 of 23 individuals). Limited vocabulary was also present in several adolescent and adult individuals (N_9, N_11, N_18, N_23, N_31, N_54, N_60). In contrast, 44% (10 of 23) used everyday speech and could form standard sentences. Individual N_59 had dyslexia and was unable to read at 19 years of age, and N_32 could neither read nor write at age 10.

ID or borderline ID was diagnosed in 29 of 39 individuals (74%). ID severity was categorized as moderate to severe in 13%, mild in 26% and borderline in 26%. In addition, three individuals were reported to have learning difficulties without ID. Formal IQ testing was available for 10 individuals aged 5 years or older (mean age 13 years; range 5-40 years), revealing a mean IQ of 70 (range 38-92).

Analysis of developmental delay, ID and speech difficulties showed no evidence of more severe involvement in males compared to females. Interestingly, six individuals with early motor and speech delays demonstrated developmental improvement over time and were reported to catch up on key milestones.

Abnormalities of the nervous system

Epilepsy or seizures were reported in 6 of 40 individuals (15%), with five (13%) having a diagnosis of epilepsy. In family F, the father (N_11) reported epilepsy onset at 5 years, and his son (N_9) was diagnosed with absence epilepsy at 2 years. N_64 had focal epilepsy and N_16

had focal to bilateral tonic-clonic seizures. One individual (N_30) showed increased seizure susceptibility on EEG without clinical seizures. In individual N_23 epilepsy type was not specified.

Brain magnetic resonance imaging (MRI) was performed in 21 individuals; 14 had normal results and 7 (33%) showed abnormalities, including partial or absent corpus callosum (n=2), perisylvian polymicrogyria (n=1), subcortical heterotopia (n=1), hydrocephalus with Chiari I malformation (n=1), diffusion restriction consistent with hypoxic-ischemic injury (n=1), reduced grey-white matter differentiation (n=1), increased CSF spaces and a thin arachnoid cyst (n=1), and new changes in the internal capsule and basal ganglia at age 15 years (n=1). Two individuals had more than one finding.

Atypical behavior

Autism or autistic traits were documented in 21 of 41 individuals with a formal diagnosis of autism in 14 individuals (34%). ADHD or attention deficit disorder (ADD) was present in 58% (14 of 24) of individuals with LoF variants, but only in 8% (1 of 12) of individuals with protein-altering-variants, a difference that was statistically significant ($p = 0.004$, Fisher's exact test). Atypical behavior was described by attending physicians in 79% (27 of 34) of individuals. Reported features included aggressive behavior (7 of 34; 21%), abnormal emotional behavior (6 of 34; 18%) and impaired social behavior (4 of 34; 11%). In addition, one girl (N_8) had abnormal stereotypical hand movements, and her brother (N_9) showed nervous encopresis.

Dysmorphic features

Facial characteristics were variable, with dysmorphic features reported in 30 of 45 individuals (67%) including 20 with LoF variants and 10 with protein-altering variants (Additional File 3: Fig. S1C). The most frequent dysmorphic features involved palpebral fissures, present in 14 of 41 individuals (34%), including upslanting (n=6), downslanting (n=5), long (n=2) and almond shaped palpebral fissures (n=1). Additional features included low-set ears (n=3) and

craniofacial features in seven individuals, such as plagiocephaly, broad forehead, and retrognathia.

GestaltMatcher analysis of facial photos from 15 CTNND2 individuals showed that 85% of the intra-cohort similarity distribution overlapped with the range of randomly sampled controls, suggesting that CTNND2 individuals, as a group, do not exhibit a consistent or distinctive facial gestalt (Fig. 1B, Additional File 3: Fig. S1A). In pairwise similarity analysis (Additional File 3: Fig. S1B), only a subset of individuals, specifically N_17 and N_17a (siblings), N_7, N_8, N_9, N_10 (another family cluster), as well as N_43 and N_23, formed a visible cluster, with patients N_58 and N_19 also showing notable similarity. These results indicate that while facial similarities exist among certain individuals, the cohort as a whole does not exhibit a consistent or distinguishable facial pattern, though larger sample sizes may be required to draw firmer conclusions. In summary, both clinical observation and computational analysis suggest that although some CTNND2 individuals display dysmorphic facial features, no distinct facial gestalt is consistently observed.

Additional symptoms

N_7, N_8, N_9 and N_10 had microcephaly during the first three years of life, with head circumference measurements below the 3rd percentile. At later follow-up examinations, the head circumference increased into the normal range although it remained on the small side in N_7, N_9, and N_10. Short stature was reported in two individuals, while all others had normal height. Ophthalmologic features were present in 20 of 46 individuals (43%). Myopia was present in 9 individuals and strabismus in five. Additionally, discrete muscular hypotonia was observed in four individuals, and hyperextensible joints in six of 39 individuals (15%).

Familial *CTNND2* Variants and Phenotypic Variability

In twelve of the previously unpublished cases, the *CTNND2* variant was inherited from an affected parent. In addition, the missense variant c.3163C>G, p.(Arg1055Gly) was identified in three siblings, and is presumed to be inherited, although parental samples were not available for testing.

Clinical manifestations varied significantly among family members carrying the same *CTNND2* variant. For example, in families D and E, the index patient had moderate ID while other family members presented with borderline ID, learning disability or no reported ID (Fig. 2A). In family F, the degree of language impairment differed between family members: the index individual (N_7) had difficulties forming sentences; his sister (N_8) had normal speech; his brother (N_9) had limited vocabulary and impaired sentence formation, with comprehension and expressive language at the age of 12 corresponding to a developmental level of 7.5 years. Another brother (N_10) had a clear articulation disorder, dyslalia and echolalia and a limited vocabulary. Their father (N_11) also had difficulties forming sentences.

In individuals with *de novo CTNND2* variants and index cases, the cognitive spectrum ranged from normal cognition to severe ID. In contrast, none of the non-index family members with an inherited *CTNND2* variant had moderate or severe ID (Fig. 2B).

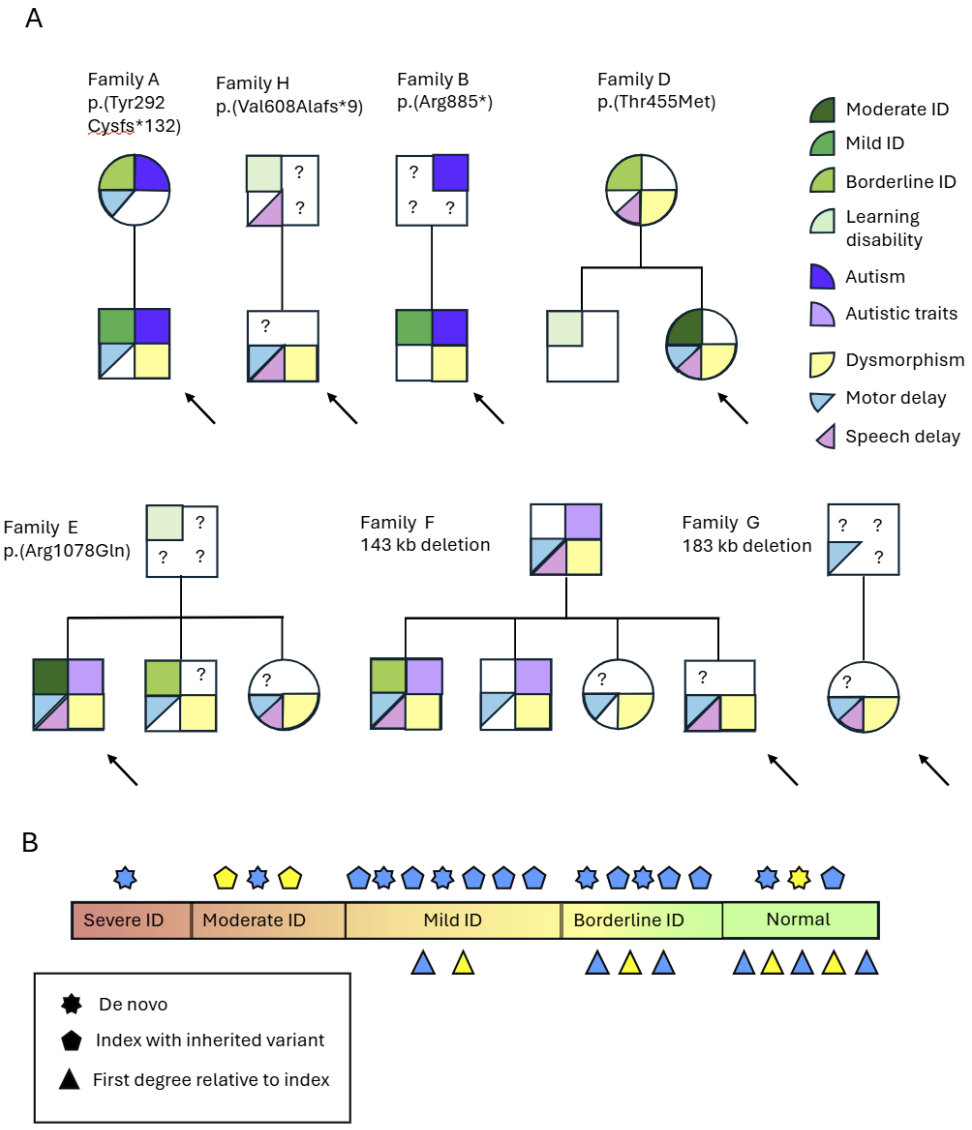


Figure 2. Familial *CTNND2* variants and phenotypic variability. A. Pedigrees of novel familial *CTNND2* cases showing the phenotypic spectrum within families carrying the same *CTNND2* variant. Arrows indicate the index case. Question marks indicate information that was not available. **B.** Distribution of cognitive function in individuals harboring familial or *de novo CTNND2* variants. Blue indicates pathogenic or likely pathogenic variants, yellow indicates variants of uncertain significance (VUS).

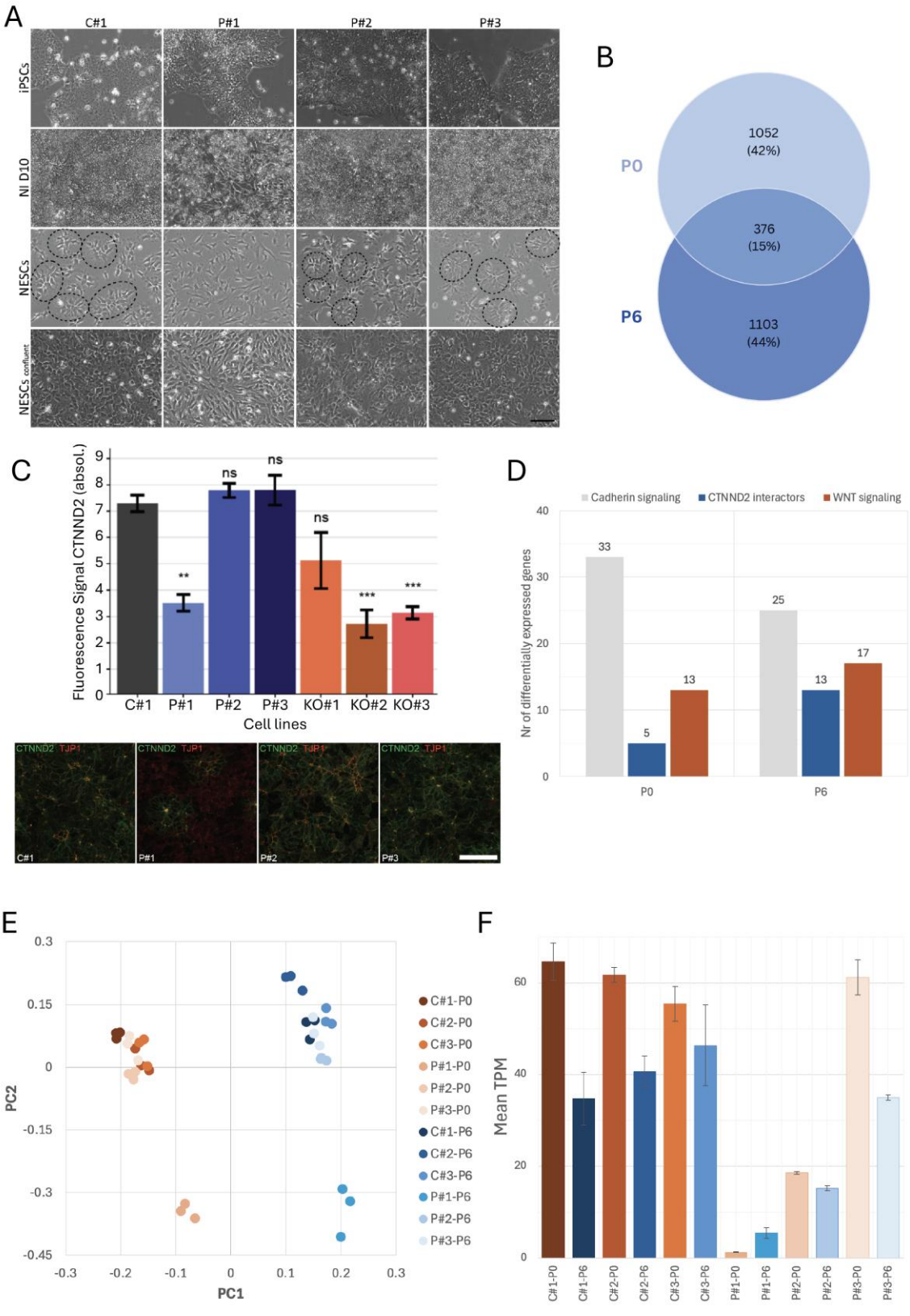
Patient-derived iPSC/NESC models reveal variable effects on early neural induction

Before neural induction, we assessed the genomic integrity of the patient-derived iPSC lines (Additional File 3: Fig. S2B, C; Additional File 1: Table S3). All clones selected for the

experiments were considered suitable for further analysis, with no additional significant chromosomal abnormalities identified. Two clones were derived from P#1. SNP-array analysis detected no reportable copy-number changes in clone ALI-07-X, which was used in all experiments, whereas clone ALI-07-II carried a gain involving 20q11.21 and was excluded. Other SNP-array findings are listed in Additional File 1: Table S3. None of the clones used in the experiments showed copy-number changes involving 12p13.31, 20q11.21 or the TP53 region, which have been reported as recurrently altered in cultured iPSCs (Amps et al., 2011; Baker et al., 2007; Martins-Taylor et al., 2011; Merkle et al., 2017). Optical genome mapping of the clones used in the experiments confirmed the known balanced translocations t(1;8) and t(5;18) in P#1 and P#2 and the *CTNND2* exon 4–9 deletion in P#3 (Additional File 3: Fig. S2B). G-banding of P#1 clone ALI-07-X confirmed the same translocations, with no additional abnormalities detected in 25 metaphases (Additional File 3: Fig. S2C).

To investigate the role of *CTNND2* in early human brain development, iPSCs from three affected individuals and three controls (Additional File 1: Table S2) were subjected to neural induction to generate NESCs. Transcriptomic analyses were performed at day 12 of neural induction (passage 0; P0) and passage 6 (established NESCs; P6) after neural induction. Bright-field analysis showed apparently normal neural induction in two of the three patient-derived lines (P#2 and P#3), whereas neural rosette formation was abnormal in P#1 (Fig. 3A). Quantification of CTNND2 immunofluorescence showed a significantly reduced signal in P#1 compared with C#1, whereas no significant difference was detected in P#2 or P#3 (Fig. 3C). RNA was collected at P0 and P6, and transcriptomic profiles clustered primarily by time point, while P#1 separated from the other lines along principal component 2 (Fig. 3E). We next quantified *CTNND2* expression in the RNA-seq data. Mean expression across the three control lines was approximately 61 TPM at P0 and 42 TPM at P6 (Fig. 3F). Relative to the control mean, *CTNND2* expression was lowest in P#1, at approximately 5% and 12% at the two time

points, followed by P#2 at 31% and 40%. P#3 showed near-normal expression, corresponding to 98% and 83% of control levels. In P#3, the deletion of exons 4–9 resulted in an aberrant, predicted non-functional transcript, visible as an exon-skipping event in the sashimi plot (Additional File 3: Fig. S3A). At P0, 3557, 1444, and 439 differentially expressed genes (DEGs) were identified in P#1, P#2, and P#3, respectively; at P6, the corresponding numbers were 3863, 942, and 1263. When the three patient-derived lines were analysed together against controls, 1428 DEGs were identified at P0 and 1479 at P6 (Fig. 3B, Additional File 1: Tables S5 and S6). CTNND2 is annotated in both the KEGG cadherin and WNT signaling pathways, and its interactome comprised 89 interactors plus CTNND2 itself (Additional File 3: Fig. S4), including four interactors shared exclusively with WNT signaling, 19 shared exclusively with cadherin signaling, and five shared with both pathways. Among the combined DEGs, 33 cadherin pathway genes, five *CTNND2* interactors, and 13 WNT pathway genes were identified at P0, compared with 25, 13, and 17 genes, respectively, at P6 (Fig. 3D). Pathway enrichment analysis showed 3.5-fold enrichment of the cadherin signaling pathway and 2.6-fold enrichment of the WNT signaling pathway at P0; the corresponding enrichments at P6 were 2.9-fold and 2.1-fold. The complete pathway enrichment results are provided in Additional File 1: Tables S7 and S8 (P0) and Tables S9 and S10 (P6).



441

442 **Figure 3. Patient-derived iPSC/NESC models reveal variable effects of *CTNND2* disruption**
443 **during early neural induction. A.** Bright-field microscopy showing the morphology of the control line
444 (C#1) and three patient-derived cell lines (P#1-3) at the iPSC stage, day 10 (D10) of neural induction
445 (NI), and during NESC culture at low and high confluency. Neural rosettes are indicated by dashed

circles. **B.** Venn diagram showing the overlap of differentially expressed genes (DEGs) identified at P0 and at P6 in the combined patient-derived-versus-control comparison. **C.** Quantification of CTNND2 immunofluorescence intensity in NESC cultures from C#1, P#1-3, and KO#1-3. For each cell line, 3–5 differentiation replicates were analysed, with nine sections quantified per replicate. Mean CTNND2 fluorescence intensity was measured using ImageJ/Fiji. Data are presented as mean ± SEM. Statistical significance was assessed using a two-sided unpaired t-test with Bonferroni correction for multiple comparisons (ns, not significant; **, $p<0.01$; ***, $p<0.001$, relative to C#1). Representative CTNND2 and TJP1 immunofluorescence images are shown below. Scale bar, 100 μm. **D.** Number of DEGs belonging to the cadherin signaling pathway, CTNND2 interactome, or WNT signaling pathway in the combined patient-derived versus control comparison at P0 and P6. **E.** Principal component analysis (PCA) of RNA-seq samples from the three patient-derived and three control lines at P0 and P6. Samples separate primarily by developmental time point, with P#1 separating from the other lines along principal component 2. **F.** Mean *CTNND2* expression (TPM) in patient-derived and control lines at P0 and P6.

Isogenic *CTNND2* Knockout lines reveal dosage-sensitive transcriptional changes

To further investigate the molecular consequences of *CTNND2* disruption in an isogenic genetic background, we generated three CRISPR–Cas9-edited *CTNND2* lines using C#1 as the parental line: one heterozygous line (KO#1) and two homozygous lines (KO#2 and KO#3; Additional File 3: Fig. S2). Initial characterization showed normal neural induction and morphology in all three knockout lines at both P0 and P6 (Fig. 4B). RNA-seq was performed at both time points. Inspection of the *CTNND2* transcripts confirmed the CRISPR-induced deletion in approximately half of the transcripts in KO#1 and in all transcripts in KO#2 and KO#3 (Fig. 4A). The introduced deletions are predicted to disrupt the reading frame and are thus likely to result in loss of functional CTNND2 protein. To assess the effect of the CRISPR-induced deletions at the protein level, CTNND2 immunofluorescence was quantified in control and knockout lines. CTNND2 immunofluorescence signal was significantly reduced in the homozygous edited lines KO#2 and KO#3 compared with C#1. The heterozygous line KO#1 showed a lower mean signal, but the difference was not statistically significant (Fig. 3C). Representative staining is shown in Fig. 4B.

Global transcriptomic analysis showed that the knockout lines clustered with the other samples primarily according to developmental time point rather than genotype. This stage-associated pattern is illustrated by the expression in knockout and patient-derived lines of the top 30 genes differentially expressed between P0 and P6 in control lines (Fig. 4F). Differential expression analysis identified 484 and 496 DEGs in the heterozygous and combined homozygous knockout lines, respectively, at P0, increasing to 922 and 1016 DEGs at P6 (Additional File 1: Tables S11-S14). Among genes showing a dosage-dependent expression pattern, 113 were upregulated in the heterozygous line and further upregulated in the homozygous lines at P0, whereas 119 were downregulated in the heterozygous line and further downregulated in the homozygous lines. At P6, the corresponding numbers were 35 and 56 genes, respectively (Table 2; Additional File 3: Fig. S5A and B). A heatmap of these dosage-sensitive genes showed that the heterozygous knockout line clustered with the patient-derived lines (Fig. 4E). In the heterozygous knockout line, the number of DEGs increased from P0 to P6, with 152 genes shared between the two time points, 12% of the total unique DEGs. Among genes differentially expressed in both heterozygous and homozygous knockout lines relative to controls, 437 were identified at P0 and 987 at P6, with 109 genes shared between the two time points (Fig. 4C). The overlap between DEGs in the heterozygous knockout and patient-derived lines was 134 genes at P0 and 431 genes at P6 (Fig. 4D).

Table 2. Dosage-dependent expression changes in *CTNND2* knockout lines.

	Het+ / Hom ++	**Het++ / Hom +**	**Het- / Hom --**	**Het-- / Hom -**	**Other**
P0	113	51	119	156	220
P6	35	49	56	143	548

Note: Het, heterozygous knockout; Hom, homozygous knockout. Genes are grouped by their expression changes relative to the control line in the two knockout lines (Additional File 3: Fig. S5). A single plus sign (+) indicates upregulation, and a single minus sign (−) indicates downregulation. Double symbols (++, −−) indicate a larger expression change in the indicated line. Het+/Hom++ and Het−/Hom−− indicate a larger change in the homozygous line, whereas Het++/Hom+ and Het−−/Hom− indicate a larger change in the heterozygous line. “Other” includes genes that do not follow these four patterns.

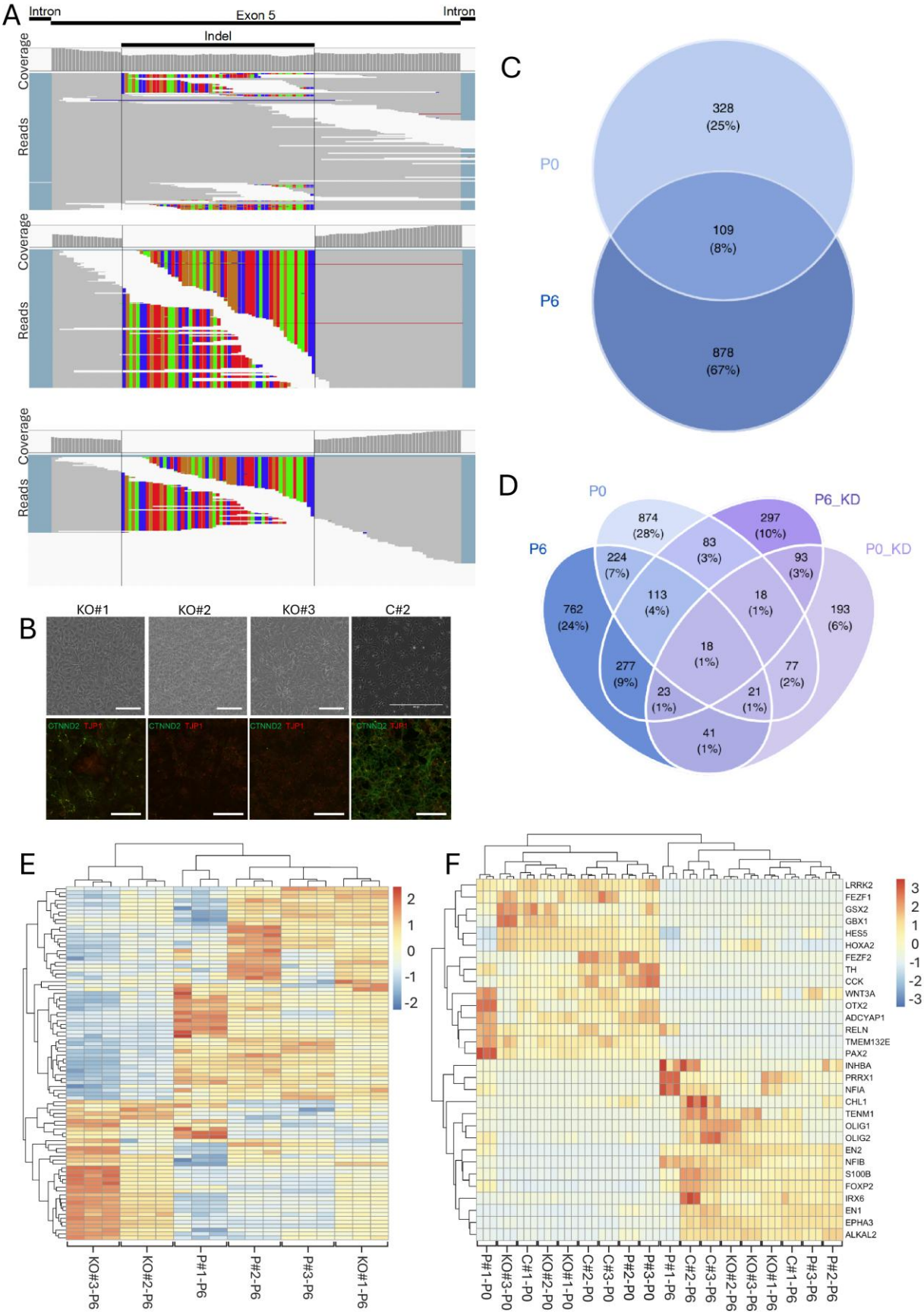


Figure 4. Isogenic *CTNND2* knockout lines reveal dosage-sensitive transcriptional changes. **A**. RNA-seq read alignment to GRCh38 and visualization in IGV showing the CRISPR-induced deletion

in *CTNND2* exon 5 in the heterozygous KO#1 line and homozygous KO#2 and KO#3 lines. **B.** Bright-field microscopy and representative immunofluorescence staining of CTNND2 and TJP1 in NESCs from KO#1–3 and control line C#2. Scale bar 100 μm, except for the C#2 bright-field image, 400 μm. **C.** Venn diagram showing the overlap of differentially expressed genes (DEGs) identified by directly comparing heterozygous and homozygous knockout lines at P0 and P6. **D.** Venn diagram showing the overlap of DEGs identified in patient-derived lines and the heterozygous *CTNND2* knockout line, each compared with controls, at P0 and P6. **E.** Heatmap of genes showing dosage-dependent expression changes, with greater upregulation or downregulation in homozygous than heterozygous knockout lines relative to controls. Expression is shown across patient-derived and knockout lines at P6. **F.** Heatmap showing expression across all cell lines at P0 and P6 of the top 30 differentially expressed genes identified by comparing the two time points in control lines.

CTNND2-associated transcriptional networks during early neural development

Finally, we explored the CTNND2 interactome together with WNT and cadherin signalling networks across the patient-derived and CRISPR-edited lines. We defined three partially overlapping gene sets: the CTNND2 interactome, WNT signaling, and cadherin signaling, comprising 89, 153, and 155 genes, respectively. The overlap included 19 genes shared between the CTNND2 interactome and cadherin signaling, 33 shared between WNT and cadherin signaling, four shared between WNT and the CTNND2 interactome, and five genes shared across all three groups (GSK3B, TCF7L2, TCF7L1, LEF1, and CTNNB1) (Additional File 3: Fig. S4). Among the differentially expressed genes in the network analysis, 28 and 26 genes were associated with the WNT signaling pathway at P0 and P6, respectively, while 29 and 21 genes were associated with the cadherin signaling pathway at P0 and P6, respectively. Network analysis showed a relatively discrete cluster of WNT-associated genes, whereas cadherin-associated genes showed greater overlap with the CTNND2 interactome (Fig. 5A and B). The network analysis also distinguished genes altered only in patient-derived lines, genes altered in both patient-derived and heterozygous CRISPR lines, and genes altered only in CRISPR lines (Fig. 5A and B).

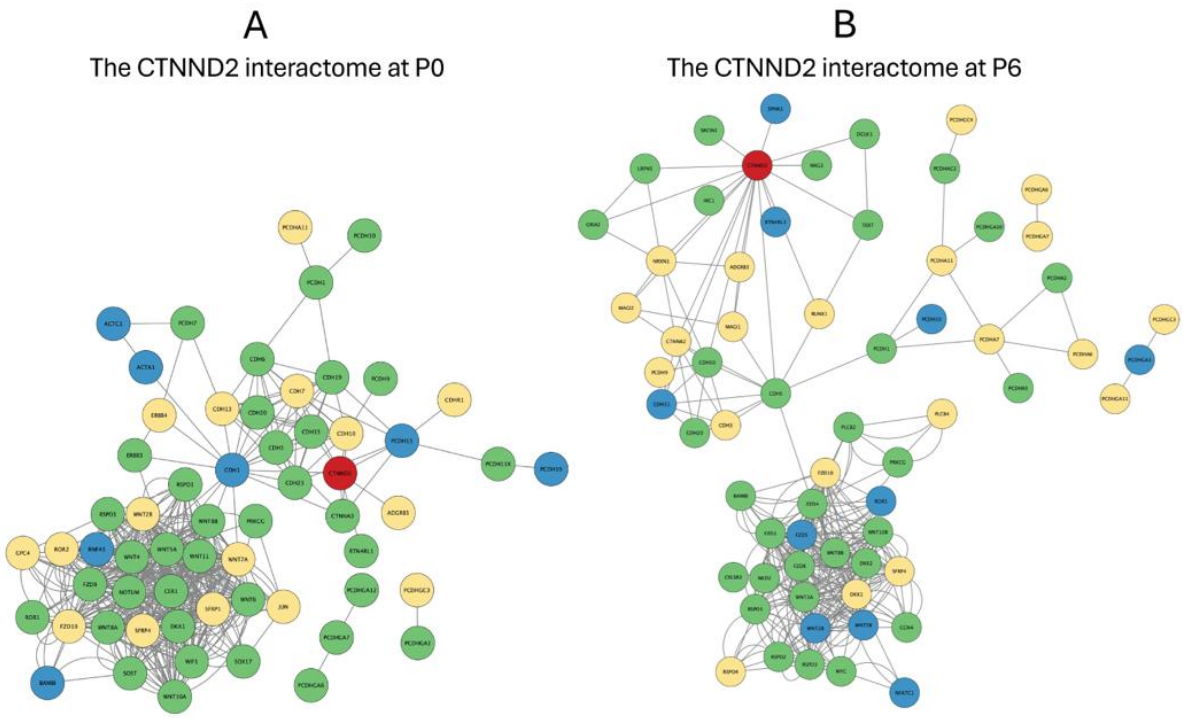


Figure 5. *CTNND2*-associated transcriptional networks during early neural development. A–B. Network analysis of differentially expressed genes within the CTNND2 interactome and WNT and cadherin signaling pathways at P0 (A) and P6 (B). Green nodes indicate genes differentially expressed only in patient-derived lines, yellow nodes indicate genes differentially expressed in both patient-derived and heterozygous CRISPR comparisons, blue nodes indicate genes differentially expressed only in CRISPR comparisons, and the red node indicates *CTNND2*. The colors indicate in which comparisons each gene is differentially expressed, but do not distinguish upregulation from downregulation. WNT-associated genes form a relatively discrete cluster, whereas cadherin-associated genes show greater overlap with the *CTNND2* interactome.

DISCUSSION

In this study, we combined detailed clinical phenotyping with functional analyses of patient-derived and isogenic CRISPR-edited iPSC models to investigate *CTNND2*-related neurodevelopmental disorders. Our cohort of 57 individuals, including 42 newly described and 15 previously reported cases, defines a core clinical spectrum characterized by intellectual

disability and behavioral abnormalities, together with variable neurological and dysmorphic features. Functional studies revealed variability between patient-derived lines, with impaired neural rosette formation in one line, whereas the other patient-derived and CRISPR-edited lines showed apparently normal neural induction. Transcriptomic analyses across patient and CRISPR-edited models identified partly convergent transcriptional alterations involving the CTNND2 interactome and WNT and cadherin signaling networks. Together, these findings provide evidence for a role for *CTNND2* in early human neural development and suggest that *CTNND2* disruption is associated with transcriptional changes across interconnected cell-adhesion and signalling networks.

This study presents the largest clinical cohort of individuals with *CTNND2* variants reported to date, revealing a broad phenotypic spectrum ranging from very mildly or borderline cognitive impairment to moderate or severe intellectual disability. This variable expressivity was also observed among individuals carrying the same familial variants. Genotype-phenotype comparisons showed a higher prevalence of ADD/ADHD among individuals with LoF variants (58%) than protein altering variants (8%; p=0.004, Fisher's exact test), raising the possibility of partially distinct mechanisms; haploinsufficiency for LoF variants versus a dominant negative or gain of function effect for protein altering variants. Alternatively, the lower frequency of ADHD/ADD observed among individuals with protein altering variants could be consistent with some variants having a hypomorphic effect, resulting in only partial loss of CTNND2 function. However, these proposed mechanisms remain speculative, as other clinical features, including intellectual disability severity, did not differ significantly between groups. The molecular consequences of individual missense variants remain unknown, and functional characterization of protein-altering variants will be required to distinguish between loss-of-function, dominant-negative, and gain-of-function effects.

Symptom severity did not differ significantly by gender. A trend toward more severe intellectual disability among *de novo* and index cases was noted (Fig. 2), although this may reflect ascertainment bias, as individuals with more severe or atypical presentations may be more likely to undergo genetic testing. Milder or subclinical cases may remain underrecognized, potentially skewing the observed distribution of phenotypic severity. Facial analysis using GestaltMatcher (Hsieh et al., 2022) did not identify a consistent facial gestalt (Fig. 1B), although some individuals showed overlapping facial features (Additional File 3: Fig. S1A and B). This further emphasizes the variable expressivity of *CTNND2*-related disorders and the challenge of clinical diagnosis. These disorders fall within the broader group of neurodevelopmental conditions characterized by intellectual disability, behavioral abnormalities, and variable neurological and cognitive features. The clinical heterogeneity observed in our cohort may reflect the complex interplay of *CTNND2* disruption with additional genetic, environmental, or epigenetic modifiers, highlighting the importance of integrating genomic data with careful clinical assessment.

Myopia was reported in 20% of assessed individuals, although the retrospective nature of the clinical data precludes a reliable comparison with the general population. Ophthalmological abnormalities are also reported in CTNNB1-related neurodevelopmental disorder (Sudnawa et al., 2024) , suggesting some phenotypic overlap, although systematic ophthalmological assessments are needed to establish the significance of these findings in *CTNND2*-related disease.

To better understand the cellular basis of the variable clinical presentations, we studied early neurogenesis in iPSC-derived models from three individuals with *CTNND2* variants. Only one patient-derived line (P#1) showed impaired neural rosette formation and failed to establish

stable NESCs, while lines from her mother (P#2) and an unrelated individual (P#3) underwent normal neural induction. The isogenic heterozygous and homozygous CRISPR-edited lines also underwent apparently normal neural induction, indicating that reduced *CTNND2* dosage alone was not sufficient to produce a consistent morphological phenotype in these models. This variability may reflect the influence of genetic background, epigenetic state, or stochastic differences during differentiation, consistent with evidence that the phenotypic consequences of disease-causing variants are shaped by factors beyond the primary mutation (Kammenga, 2017). Transcriptomic analysis further showed that P#1 was an outlier relative to the other patient-derived and CRISPR-edited lines, and subsequent analyses therefore focused on transcriptional changes shared across models rather than on the P#1-specific profile.

Transcriptomic analyses across the patient-derived and CRISPR-edited lines revealed transcriptional changes involving WNT and cadherin signaling pathways as well as the CTNND2 interactome. Differentially expressed genes were enriched in both WNT and cadherin signaling pathways, and a subset also belonged to the CTNND2 interactome, indicating that *CTNND2* disruption is associated with changes across interconnected gene networks involved in cell adhesion and neural development. These changes were observed at both P0 and P6, although the number and identity of affected genes differed between developmental stages, suggesting that the transcriptional consequences of *CTNND2* disruption vary during neural differentiation. The CRISPR-edited lines further showed dosage-dependent expression changes, with a subset of genes displaying progressively stronger dysregulation in heterozygous and homozygous knockout lines. Network analysis demonstrated a relatively discrete cluster of WNT-associated genes, whereas cadherin-associated genes showed extensive overlap with the CTNND2 interactome, consistent with the established role of δ-catenin at the interface between cell adhesion and intracellular signaling. Together, these findings support convergent

transcriptional effects of *CTNND2* disruption across patient-derived and isogenic models. Further studies at the protein and functional levels will be required to determine whether these expression changes result in altered pathway activity or directly contribute to early human neurodevelopment.

Neural rosette formation is a critical morphogenetic process during early neural differentiation *in vitro*, reflecting aspects of early neuroepithelial organization and neural stem cell development. These structures recapitulate key features of the early neuroepithelial architecture that is tightly regulated *in vivo* to maintain the proper development of neural stem cells (Malchenko et al., 2014)(Elkabetz et al., 2008). In our study, P#1 showed delayed rosette formation during neural induction, whereas the other patient-derived and CRISPR-edited lines underwent neural induction comparable to that of the control lines. This variability indicates that *CTNND2* disruption can affect early neural organization in some genetic contexts but is not sufficient to produce a consistent morphological phenotype. The enrichment of WNT and cadherin signaling genes among the differentially expressed genes nevertheless suggests that *CTNND2* disruption is associated with transcriptional changes in networks involved in neural patterning, cell adhesion, and progenitor organization.

Despite carrying *CTNND2*-disruptive alleles, the CRISPR-Cas9-generated knockout lines showed apparently normal neural induction and neural rosette formation, resembling P#2, P#3, and the control lines. Nevertheless, transcriptomic analysis identified differential expression in both heterozygous and homozygous knockout lines, indicating molecular consequences of *CTNND2* disruption despite the absence of an overt morphological phenotype. RNA-seq also detected residual *CTNND2* transcripts containing the induced indel, possibly reflecting the use of alternative downstream start codons. These transcripts are predicted to be non-functional or

partially functional, as the coding sequence was disrupted. Such incomplete gene disruption, referred to as “knockout escape”, has been described previously both in zebrafish and human iPSC models (Anderson et al., 2017; Sebastian et al., 2023) and reflects the limitations of CRISPR-based models in fully capturing the complexity of human disease (Wang et al., 2024). Patient-derived lines retain the broader genetic background in which the disease-associated variant occurs and may therefore capture modifying effects that are absent from isogenic knockout models. However, among the three patient lines included here, a clear morphological abnormality was observed only in P#1. Such variability is not unique to *CTNND2*. Similar heterogeneity has been reported in iPSC-based models of other neurodevelopmental disorders. For example, in 16p11.2 deletion models, ventral forebrain organoids exhibited significantly greater variation in size and rosette formation, with some cultures producing very few rosettes (Fetit et al., 2023). Similarly, in ASD iPSC models, some patient-derived lines show pronounced neural rosette abnormalities, whereas others appear unaffected (Adhya et al., 2021). This variability underscores the need for larger numbers of independently derived cell lines to distinguish reproducible disease-associated effects from those influenced by genetic background, clonal variation, or variability during neural induction and NESC generation.

Based on these findings, we propose a model in which *CTNND2* disruption is associated with transcriptional changes across three partially overlapping molecular networks: the CTNND2 interactome, WNT signaling, and cadherin signaling (Fig. 5A and B). The relative transcriptional effects on these networks differed between P0 and P6, suggesting that the consequences of *CTNND2* disruption are developmentally dynamic and vary during NESC generation and expansion. At P0, the changes may predominantly affect pathways involved in neural induction, cell–cell adhesion, and early progenitor organization, whereas the altered expression observed at P6 may reflect effects on NESC maintenance and expansion. This model

provides a framework for integrating the transcriptomic findings but will require validation at the protein and functional levels.

Together with previous observations, these findings highlight the need for caution when interpreting gene disruption models, as knockout alone may not fully capture the complexity of human disease phenotypes. Across the patient-derived and CRISPR-edited lines, transcriptomic analyses identified partially convergent transcriptional changes involving the CTNND2 interactome and WNT and cadherin signaling networks, despite substantial variability between individual lines and between P0 and P6. The broader clinical cohort demonstrated that *CTNND2*-related disease is associated with a highly variable neurodevelopmental phenotype, ranging from mild to severe. This variability underscores the influence of additional genetic, environmental, and epigenetic modifiers on disease severity. Our findings place *CTNND2* alongside other WNT-regulating genes such as *APC*, *CHD8*, and *CTNNB1*, whose disruption similarly causes variable neurodevelopmental disorders (de Ligt et al., 2012; Krumm et al., 2015; Nakagawa et al., 2017). Collectively, these conditions have been discussed in the context of neurodevelopmental disorders involving dysregulated WNT signaling, highlighting the critical role of finely tuned WNT signaling in early brain development (Pascual et al., 2025).

Limitations. Several limitations of this study should be acknowledged. First, although RNA-seq identified dysregulation of WNT and cadherin pathway genes, this finding has not yet been validated by qPCR or at the protein level. Second, each patient-derived and CRISPR-edited line was represented by a single reprogrammed or edited clone; independently generated biological replicate lines (particularly for P#1) would strengthen confidence that observed phenotypes reflect genotype. Finally, the functional analyses were based on a small number of patient-derived and CRISPR-edited lines; a larger sample size, including additional patient lines and

replicate clones, would improve the statistical power and generalizability of these cellular findings.

CONCLUSIONS

This study defines *CTNND2*-related neurodevelopmental disorders as clinically variable disorders characterized by intellectual disability and behavioral abnormalities. Through international collaboration, we present genotype and phenotype data from 57 individuals, providing the largest clinical cohort to date for *CTNND2*-related diseases. Functional analyses of patient-derived and CRISPR-edited iPSC-derived neural models support a role for CTNND2 in early neural development and reveal transcriptional alterations involving the CTNND2 interactome and WNT and cadherin signaling networks. The variability observed across both the clinical cohort and the cellular models suggests that the consequences of *CTNND2* disruption are influenced by genetic background and other modifying factors. Together, our findings expand the clinical and molecular spectrum of *CTNND2*-related disease and highlight the importance of coordinated cell-adhesion and signaling networks during early human neurodevelopment.

ABBREVIATIONS

ADD: Attention-Deficit Disorder.

ADHD: Attention-Deficit/Hyperactivity Disorder

iPSCs: induced pluripotent stem cells

LoF: Loss of Function

NDDs: Neurodevelopmental disorders

NESCs: Neuroepithelial stem cells

OGM: Optical genome mapping

VUS: variants of uncertain significance

DECLARATIONS

Acknowledgments

We express our sincere gratitude to the individuals and their families whose participation made this study possible. The authors acknowledge support from the National Genomics Infrastructure in Stockholm funded by Science for Life Laboratory, the Knut and Alice Wallenberg Foundation and the Swedish Research Council, and NAISS/SNIC/Uppsala Multidisciplinary Center for Advanced Computational Science for assistance with massively parallel sequencing and access to the UPPMAX computational infrastructure. This work was partly performed at the Karolinska Genome Engineering (KGE) and iPSCore facilities at Karolinska Institutet. We thank them for their technical support. We thank the Cell and Gene Therapy Core at Lund University for performing the genotype analysis and molecular karyotyping analysis that contributed to this study. Several authors in this publication are members of the European Reference Network of Rare Congenital Malformations and Rare Intellectual Disability ERN-ITHACA (EU Framework Partnership Agreement ID: 3HP-FPA ERN-01-2016/739516)

Funding

Financial support was provided to AL by grants from the Swedish Research Council (2019-02078), Hjärnfonden/the Swedish Brain Foundation (FO2022-0256) and the Swedish Rare Diseases Foundation; to AF from VR (2019-01498, 2022-00899), Hjärnfonden/the Swedish Brain Foundation (FO2019-0246, FO2021-0234, FO2022-0315), VINNOVA (IndiCell 2021-02695), Cancerfonden (20 1159 Pj) and to AN from the Swedish Research Council (2021-

02860), Hållsten research foundation and Hjärnfonden/the Swedish Brain Foundation (FO2021-0177). Part of this work was supported by a grant from the US National Human Genome Research Institute (NHGRI; UM1HG007301) to Susan Hiatt, and by MIUR project "Dipartimenti di Eccellenza 2023-2027" to the Department of Neurosciences "Rita Levi Montalcini" (University of Turin) to Alfredo Brusco.

Availability of data and materials

RNA-Seq data have been deposited in the European Genome-phenome Archive (EGA) under the accession number EGA50000000309 and are available upon request. Clinical and variant data for all individuals are provided in Additional File 1: Table S1. Other supporting data are provided in Additional Files 1–3

Author contributions

Study design: MS, RR, AF, DW, AL.

Stem cell experiments: MS, JS.

Bioinformatic analysis: JS, MS, JE.

Facial image analysis: TCH, AK, PK, JML.

Data interpretation: MS, JS, JE, AFi, RR, AF, JW, DW, AL, HTH, ME, LD.

Clinical data analysis: DW, JW, AN, AL.

Figures, tables, graphics: JS, MS, JW, RR, AS, TCH, AK, PK.

Manuscript writing: MS, JS, JE, JW, DW, AL.

Manuscript critical review: MS, JW, JE, AS, AN, AL, AF, DW.

Manuscript supervision: AL, AF, MS, DW.

Clinical data collection and review: KK, GW, SG, CM, FR, LP, AB, GM, ST, FP, BG, QW, JMvH, EB, KI, LG, AP, RO, MH, FD, EBB, SJ, GB, MJZ, CL, GMR, GJ, CK, MG, WKC,

HM, SMH, WVK, AFö, LO, ASh, BD, SM, BC, CE, ED, GR, TS, HHA, TC, ASP, JAB, VKP, FDV, JTA, IT, EGF, ASAC, SW, HCD.

All authors have read and approved the final version of the manuscript.

Ethics approval and consent to participate.

Written informed consent for genetic testing and publication of clinical information was obtained from the affected individual or legal guardians in accordance with the Declaration of Helsinki. Ethical approval for this study was granted by the regional ethical review board in Stockholm Sweden (2012/2106-31/4 and 2016/430-31), and the ethics committee at the Johannes Kepler University Linz (ECS 1253/2021).

Competing interests

The authors declare that they have no competing interests.

Supplementary Information

Additional File 1: Table S1. Detailed clinical information. **Table S2**. Cell lines descriptions. **Table S3.** SNP-array results of the patient-derived iPSC lines. **Table S4**. Antibodies for immunofluorescence. **Tables S5–S6.** Differentially expressed genes (DEGs) in patient-derived lines versus controls at P0 and P6. **Tables S7–S10.** Pathway enrichment results for patient-derived lines versus controls at P0 and P6. **Tables S11–S14.** Differentially expressed genes (DEGs) from heterozygous and homozygous *CTNND2* knockout lines at P0 and P6.

Additional File 2: Supplementary Methods

Additional File 3: Figures S1–S5

Figure S1. GestaltMatcher analysis of facial features in individuals with *CTNND2* variants. A. Distance distribution comparison among CTNND2 individuals and controls. The distance distribution among CTNND2 patients is depicted in orange, the random selection from subjects with 328 disorders is shown in red, and the selection with the same disorder is illustrated in blue. The black vertical line represents the threshold distinguishing syndrome-specific from random distributions. In this analysis, 85% of the *CTNND2* distribution falls above the threshold, suggesting that CTNND2 individuals do not exhibit a consistent facial gestalt. **B.** GestaltMatcher pairwise rank analysis. The pairwise rank matrix displays the matched rank within a gallery of 7,459 images representing 449 syndromes. Lower rank values (dark blue) indicate higher facial similarity. For instance, consider column N_23: Patient N_8 is ranked 4th (i.e., the 4th most similar image) among the 7,459 images in the gallery, indicating a relatively high facial similarity between these two individuals. Some localized similarity was observed within the cohort, including among individuals from the same families (N_7–N_10 and N_17/N_17a) but no consistent similarity pattern was observed across the cohort. **C.** Facial photographs of 18 individuals with *CTNND2* variants, illustrating the range of facial features observed across affected individuals. Of these, 15 were included in the GestaltMatcher analysis; N_20, N_21, and N_42 were excluded.

Figure S2. iPSC knockout lines and **quality control of iPSC lines: optical genome mapping and G-banding. A.** KO#1-#3 was cultured on laminin 521. Colonies of each cell line showed the smooth cell edges typical for iPSC cultures, scale bar 400 µm. **B.** Optical genome mapping of the patient-derived iPSC lines. Circos plots of P#1 (I) and P#2 (II) show the balanced translocations t(1;8) and t(5;18). Genome browser view (III) of the 143 kb deletion in *CTNND2* (exons 4–9) in P#3. **C.** G-banding karyogram of P#1 (clone ALI-07-X) showing 46,XX,t(1;8)(p22;q24),t(5;18)(p15;q11). The translocated chromosomes are indicated.

Figure S3. Aberrant *CTNND2* transcript structure in patient-derived line P#3. A. Sashimi plot of RNA-seq reads across CTNND2 in P#3 and a control, showing the deletion of exons 4–9 and the resulting exon-skipping event in the *CTNND2* transcript of P#3. **B.** RNA-seq read distribution at a heterozygous *CTNND2* single-nucleotide variant (SNV) showing approximately balanced representation of the two alleles, with no evidence of marked allelic expression imbalance.

Figure S4. CTNND2 interactome and its overlap with WNT and cadherin signaling networks. Network of the CTNND2 interactome, with CTNND2 shown in grey, together with the genes of the WNT and cadherin signaling pathways. Orange nodes are CTNND2 interactors that are not part of either pathway. Yellow nodes are interactors shared only with WNT signaling (n = 4), pink nodes are shared only with cadherin signaling (n = 19), and red nodes are shared with both pathways (n = 5). Green nodes are WNT pathway genes and blue nodes are cadherin pathway genes that are not CTNND2 interactors.

Figure S5. Dosage-dependent expression changes in *CTNND2* knockout lines. A–B. Scatter plots showing the relationship between gene expression changes in heterozygous and homozygous *CTNND2* knockout lines relative to the control line at P0 (A) and P6 (B). Genes are categorized according to their dosage-dependent expression patterns. Colours correspond to the columns of Table 2: upregulated in both lines, more strongly upregulated in Hom (Het+/Hom++ red); upregulated in both lines, more strongly upregulated in Het (Het++/Hom+ olive); downregulated in both lines, more strongly downregulated in Hom (Het−/Hom−− green); and downregulated in both lines, more strongly downregulated in Het (Het−−/Hom− blue). Genes that do not follow these four patterns are shown as Other (pink). The dashed line marks equal log2 fold change in both lines.

REFERENCES

Adegbola, A., Lutz, R., Nikkola, E., Strom, S. P., Picker, J., & Wynshaw-Boris, A. (2020). Disruption of CTNND2, encoding delta-catenin, causes a penetrant attention deficit disorder and myopia. *Human Genetics and Genomics Advances*, *1*(1). https://doi.org/10.1016/j.xhgg.2020.100007

Adhya, D., Swarup, V., Nagy, R., Dutan, L., Shum, C., Valencia-Alarcón, E. P., Jozwik, K. M., Mendez, M. A., Horder, J., Loth, E., Nowosiad, P., Lee, I., Skuse, D., Flinter, F. A., Murphy, D., McAlonan, G., Geschwind, D. H., Price, J., Carroll, J., … Baron-Cohen, S. (2021). Atypical Neurogenesis in Induced Pluripotent Stem Cells From Autistic Individuals. *Biological Psychiatry*, *89*(5), 486–496. https://doi.org/10.1016/j.biopsych.2020.06.014

Ambrose, A., McNiven, V., Wilson, D., Tempes, A., Underwood, M., Chau, V., Schulze, A., Wyszynska, A., Desch, K., Malik, A. R., & Mercimek-Andrews, S. (2025). Neonatal Encephalopathy: Novel Phenotypes and Genotypes Identified by Genome Sequencing. *Neurology: Genetics*, *11*(1). https://doi.org/10.1212/NXG.0000000000200232

Amps, K., Andrews, P. W., Anyfantis, G., Armstrong, L., Avery, S., Baharvand, H., Baker, J., Baker, D., Munoz, M. B., Beil, S., Benvenisty, N., Ben-Yosef, D., Biancotti, J. C., Bosman, A., Brena, R. M., Brison, D., Caisander, G., Camarasa, M. V., Chen, J., … Zhou, Q. (2011). Screening ethnically diverse human embryonic stem cells identifies a chromosome 20 minimal amplicon conferring growth advantage. *Nature Biotechnology*, *29*(12). https://doi.org/10.1038/nbt.2051

Anderson, J. L., Mulligan, T. S., Shen, M. C., Wang, H., Scahill, C. M., Tan, F. J., Du, S. J., Busch-Nentwich, E. M., & Farber, S. A. (2017). mRNA processing in mutant zebrafish lines generated by chemical and CRISPR-mediated mutagenesis produces unexpected transcripts that escape nonsense-mediated decay. *PLoS Genetics*, *13*(11). https://doi.org/10.1371/journal.pgen.1007105

Arikkath, J., Israely, I., Tao, Y., Mei, L., Liu, X., & Reichardt, L. F. (2008). Erbin controls dendritic morphogenesis by regulating localization of δ-catenin. *Journal of Neuroscience*, *28*(28), 7047–7056. https://doi.org/10.1523/JNEUROSCI.0451-08.2008

Arikkath, J., Peng, I. F., Yu, G. N., Israely, I., Liu, X., Ullian, E. M., & Reichardt, L. F. (2009). Δ-Catenin Regulates Spine and Synapse Morphogenesis and Function in Hippocampal Neurons During Development. *Journal of Neuroscience*, *29*(17), 5435–5442. https://doi.org/10.1523/JNEUROSCI.0835-09.2009

Asadollahi, R., Oneda, B., Joset, P., Azzarello-Burri, S., Bartholdi, D., Steindl, K., Vincent, M., Cobilanschi, J., Sticht, H., Baldinger, R., Reissmann, R., Sudholt, I., Thiel, C. T., Ekici, A. B., Reis, A., Bijlsma, E. K., Andrieux, J., Dieux, A., FitzPatrick, D., … Rauch, A. (2014). The clinical significance of small copy number variants in neurodevelopmental disorders. *Journal of Medical Genetics*, *51*(10). https://doi.org/10.1136/jmedgenet-2014-102588

Baker, D. E. C., Harrison, N. J., Maltby, E., Smith, K., Moore, H. D., Shaw, P. J., Heath, P. R., Holden, H., & Andrews, P. W. (2007). Adaptation to culture of human embryonic stem cells and oncogenesis in vivo. *Nature Biotechnology*, *25*(2). https://doi.org/10.1038/nbt1285

Belcaro, C., Dipresa, S., Morini, G., Pecile, V., Skabar, A., & Fabretto, A. (2015). CTNND2 deletion and intellectual disability. *Gene*, *565*(1), 146–149. https://doi.org/10.1016/j.gene.2015.03.054

Calvo-Garrido, J., Winn, D., Maffezzini, C., Wedell, A., Freyer, C., Falk, A., & Wredenberg, A. (2021). Protocol for the derivation, culturing, and differentiation of human iPS-cell-

derived neuroepithelial stem cells to study neural differentiation in vitro. *STAR Protocols*, *2*(2), 100528. https://doi.org/10.1016/j.xpro.2021.100528

Chen, Z., Li, X., Cui, X., Zhang, L., Liu, Q., Lu, Y., Wang, X., Shi, H., Ding, M., Yang, Y., Li, W., & Lv, L. (2023). Association of CTNND2 gene polymorphism with schizophrenia: Two-sample case-control study in Chinese Han population. *International Journal of Psychiatry in Medicine*, *58*(5). https://doi.org/10.1177/00912174231164669

de Ligt, J., Willemsen, M. H., van Bon, B. W. M., Kleefstra, T., Yntema, H. G., Kroes, T., Vulto-van Silfhout, A. T., Koolen, D. A., de Vries, P., Gilissen, C., del Rosario, M., Hoischen, A., Scheffer, H., de Vries, B. B. A., Brunner, H. G., Veltman, J. A., & Vissers, L. E. L. M. (2012). Diagnostic Exome Sequencing in Persons with Severe Intellectual Disability. *New England Journal of Medicine*, *367*(20), 1921–1929. https://doi.org/10.1056/nejmoa1206524

Dobin, A., Davis, C. A., Schlesinger, F., Drenkow, J., Zaleski, C., Jha, S., Batut, P., Chaisson, M., & Gingeras, T. R. (2013). STAR: Ultrafast universal RNA-seq aligner. *Bioinformatics*, *29*(1), 15–21. https://doi.org/10.1093/bioinformatics/bts635

Elkabetz, Y., Panagiotakos, G., Al Shamy, G., Socci, N. D., Tabar, V., & Studer, L. (2008). Human ES cell-derived neural rosettes reveal a functionally distinct early neural stem cell stage. *Genes & Development*, *22*(2), 152–165. https://doi.org/10.1101/gad.1616208

Ewels, P., Peltzer, A., Fillinger, S., Patel, H., Alneberg, J., Gracia, M. U., Di Tommaso, P., & Nahnsen, S. (2020). The nf-core framework for community-curated bioinformatics pipelines. *Nature Biotechnology*, *38*(3), 272–276. https://doi.org/10.1038/s41587-020-0446-y

Fetit, R., Barbato, M. I., Theil, T., Pratt, T., & Price, D. J. (2023). 16p11.2 deletion accelerates subpallial maturation and increases variability in human iPSC-derived ventral telencephalic organoids. *Development (Cambridge)*, *150*(4). https://doi.org/10.1242/dev.201227

Hofmeister, W., Nilsson, D., Topa, A., Anderlid, B.-M., Darki, F., Matsson, H., Tapia Páez, I., Klingberg, T., Samuelsson, L., Wirta, V., Vezzi, F., Kere, J., Nordenskjöld, M., Syk Lundberg, E., & Lindstrand, A. (2015). *CTNND2* —a candidate gene for reading problems and mild intellectual disability. *Journal of Medical Genetics*, *52*(2), 111–122. https://doi.org/10.1136/jmedgenet-2014-102757

Hsieh, T. C., Bar-Haim, A., Moosa, S., Ehmke, N., Gripp, K. W., Pantel, J. T., Danyel, M., Mensah, M. A., Horn, D., Rosnev, S., Fleischer, N., Bonini, G., Hustinx, A., Schmid, A., Knaus, A., Javanmardi, B., Klinkhammer, H., Lesmann, H., Sivalingam, S., … Krawitz, P. M. (2022). GestaltMatcher facilitates rare disease matching using facial phenotype descriptors. *Nature Genetics*, *54*(3), 349–357. https://doi.org/10.1038/S41588-021-01010-X

Hustinx, A., Hellmann, F., Sümer, Ö., Javanmardi, B., André, E., Krawitz, P., & Hsieh, T.-C. (2023). *Improving Deep Facial Phenotyping for Ultra-rare Disorder Verification Using Model Ensembles*. https://doi.org/10.1109/WACV56688.2023.00499

Ioannidis, N. M., Rothstein, J. H., Pejaver, V., Middha, S., McDonnell, S. K., Baheti, S., Musolf, A., Li, Q., Holzinger, E., Karyadi, D., Cannon-Albright, L. A., Teerlink, C. C., Stanford, J. L., Isaacs, W. B., Xu, J., Cooney, K. A., Lange, E. M., Schleutker, J., Carpten, J. D., … Sieh, W. (2016). REVEL: An Ensemble Method for Predicting the Pathogenicity of Rare Missense Variants. *American Journal of Human Genetics*, *99*(4), 877–885. https://doi.org/10.1016/j.ajhg.2016.08.016

Israely, I., Costa, R. M., Xie, C. W., Silva, A. J., Kosik, K. S., & Liu, X. (2004). Deletion of the Neuron-Specific Protein Delta-Catenin Leads to Severe Cognitive and Synaptic Dysfunction. *Current Biology*, *14*(18), 1657–1663. https://doi.org/10.1016/j.cub.2004.08.065

945 Kammenga, J. E. (2017). The background puzzle: how identical mutations in the same gene
946 lead to different disease symptoms. *FEBS Journal*, *284*(20), 3362–3373.
947 https://doi.org/10.1111/FEBS.14080
948 Kanehisa, M., Sato, Y., Kawashima, M., Furumichi, M., & Tanabe, M. (2016). KEGG as a
949 reference resource for gene and protein annotation. *Nucleic Acids Research*, *44*(D1),
950 D457–D462. https://doi.org/10.1093/nar/gkv1070
951 Kele, M., Day, K., Rönnholm, H., Schuster, J., Dahl, N., & Falk, A. (2016). Generation of
952 human iPS cell line CTL07-II from human fibroblasts, under defined and xeno-free
953 conditions. *Stem Cell Research*, *17*(3), 474–478.
954 https://doi.org/10.1016/j.scr.2016.09.028
955 Kim, H., Han, J.-R., Park, J., Oh, M., James, S. E., Chang, S., Lu, Q., Lee, K. Y., Ki, H.,
956 Song, W.-J., & Kim, K. (2008a). Delta-catenin-induced dendritic morphogenesis. An
957 essential role of p190RhoGEF interaction through Akt1-mediated phosphorylation. *The*
958 *Journal of Biological Chemistry*, *283*(2), 977–987.
959 https://doi.org/10.1074/jbc.M707158200
960 Kim, H., He, Y., Yang, I., Zeng, Y., Kim, Y., Seo, Y.-W., Murnane, M. J., Jung, C., Lee, J.-
961 H., Min, J.-J., Kwon, D.-D., Kim, K. K., Lu, Q., & Kim, K. (2012). δ-Catenin promotes
962 E-cadherin processing and activates β-catenin-mediated signaling: Implications on
963 human prostate cancer progression. *Biochimica et Biophysica Acta (BBA) - Molecular*
964 *Basis of Disease*, *1822*(4), 509–521. https://doi.org/10.1016/j.bbadis.2011.12.015
965 Kim, H., Oh, M., Lu, Q., & Kim, K. (2008b). E-Cadherin negatively modulates δ-catenin-
966 induced morphological changes and RhoA activity reduction by competing with
967 p190RhoGEF for δ-catenin. *Biochemical and Biophysical Research Communications*,
968 *377*(2), 636–641. https://doi.org/10.1016/j.bbrc.2008.10.030
969 Kim, K., Sirota, A., Chen, Y. H., Jones, S. B., Dudek, R., Lanford, G. W., Thakore, C., & Lu,
970 Q. (2002). Dendrite-like process formation and cytoskeletal remodeling regulated by δ-
971 catenin expression. *Experimental Cell Research*, *275*(2), 171–184.
972 https://doi.org/10.1006/excr.2002.5503
973 Kirchhoff, A., Hustinx, A., Javanmardi, B., Hsieh, T. C., Brand, F., Hellmann, F., Mertes, S.,
974 André, E., Moosa, S., Schultz, T., Solomon, B. D., & Krawitz, P. (2025). GestaltGAN:
975 synthetic photorealistic portraits of individuals with rare genetic disorders. *European*
976 *Journal of Human Genetics*, *33*(3), 377–382. https://doi.org/10.1038/s41431-025-01787-
977 z
978 Krumm, N., Turner, T. N., Baker, C., Vives, L., Mohajeri, K., Witherspoon, K., Raja, A.,
979 Coe, B. P., Stessman, H. A., He, Z. X., Leal, S. M., Bernier, R., & Eichler, E. E. (2015).
980 Excess of rare, inherited truncating mutations in autism. *Nature Genetics*, *47*(6), 582–
981 588. https://doi.org/10.1038/ng.3303
982 Lesmann, H., Hustinx, A., Moosa, S., Klinkhammer, H., Marchi, E., Caro, P., Abdelrazek, I.
983 M., Pantel, J. T., Ten Hagen, M., Thong, M.-K., Binti Mazlan, R. A., Tae, S. K.,
984 Kamphans, T., Meiswinkel, W., Li, J.-M., Javanmardi, B., Knaus, A., Uwineza, A.,
985 Knopp, C., … Hsieh, T.-C. (2024). GestaltMatcher Database - A global reference for
986 facial phenotypic variability in rare human diseases. *MedRxiv : The Preprint Server for*
987 *Health Sciences*. https://doi.org/10.1101/2023.06.06.23290887
988 Love, M. I., Huber, W., & Anders, S. (2014). Moderated estimation of fold change and
989 dispersion for RNA-seq data with DESeq2. *Genome Biology*, *15*(12).
990 https://doi.org/10.1186/s13059-014-0550-8
991 Mak, C. C. Y., Klinkhammer, H., Choufani, S., Reko, N., Christman, A. K., Pisan, E., Chui,
992 M. M. C., Lee, M., Leduc, F., Dempsey, J. C., Sanchez-Lara, P. A., Bombei, H. M.,
993 Bernat, J. A., Faivre, L., Tran Mau-Them, F., Palafoll, I. V., Canham, N., Sarkar, A.,
994 Zarate, Y. A., … Chung, B. H. Y. (2025). Artificial intelligence-driven genotype-

epigenotype-phenotype approaches to resolve challenges in syndrome diagnostics. *EBioMedicine*, *115*, 105677. https://doi.org/10.1016/j.ebiom.2025.105677

Malchenko, S., Xie, J., de Fatima Bonaldo, M., Vanin, E. F., Bhattacharyya, B. J., Belmadani, A., Xi, G., Galat, V., Goossens, W., Seftor, R. E. B., Tomita, T., Crispino, J., Miller, R. J., Bohn, M. C., Hendrix, M. J. C., & Soares, M. B. (2014). Onset of rosette formation during spontaneous neural differentiation of hESC and hiPSC colonies. *Gene*, *534*(2), 400–407. https://doi.org/10.1016/j.gene.2013.07.101

Martins-Taylor, K., Nisler, B. S., Taapken, S. M., Compton, T., Crandall, L., Montgomery, K. D., Lalande, M., & Xu, R. H. (2011). Recurrent copy number variations in human induced pluripotent stem cells. In *Nature Biotechnology* (Vol. 29, Number 6). https://doi.org/10.1038/nbt.1890

Matter, C., Pribadi, M., Liu, X., & Trachtenberg, J. T. (2009). δ-Catenin Is Required for the Maintenance of Neural Structure and Function in Mature Cortex In Vivo. *Neuron*, *64*(3), 320–327. https://doi.org/10.1016/j.neuron.2009.09.026

Merkle, F. T., Ghosh, S., Kamitaki, N., Mitchell, J., Avior, Y., Mello, C., Kashin, S., Mekhoubad, S., Ilic, D., Charlton, M., Saphier, G., Handsaker, R. E., Genovese, G., Bar, S., Benvenisty, N., McCarroll, S. A., & Eggan, K. (2017). Human pluripotent stem cells recurrently acquire and expand dominant negative P53 mutations. *Nature*, *545*(7653), 229–233. https://doi.org/10.1038/nature22312

Mi, H., Lazareva-Ulitsky, B., Loo, R., Kejariwal, A., Vandergriff, J., Rabkin, S., Guo, N., Muruganujan, A., Doremieux, O., Campbell, M. J., Kitano, H., & Thomas, P. D. (2005). The PANTHER database of protein families, subfamilies, functions and pathways. *Nucleic Acids Research*, *33*, 284–288. https://doi.org/10.1093/nar/gki078

Miller, D. E., Squire, A., & Bennett, J. T. (2020). A child with autism, behavioral issues, and dysmorphic features found to have a tandem duplication within CTNND2 by mate-pair sequencing. *American Journal of Medical Genetics, Part A*, *182*(3). https://doi.org/10.1002/ajmg.a.61442

Nakagawa, N., Li, J., Yabuno-Nakagawa, K., Eom, T. Y., Cowles, M., Mapp, T., Taylor, R., & Anton, E. S. (2017). APC sets the Wnt tone necessary for cerebral cortical progenitor development. *Genes and Development*, *31*(16). https://doi.org/10.1101/gad.302679.117

Pascual, D. M., Rizi, D. J., Kaur, H., & Marcogliese, P. C. (2025). Excess Wnt in neurological disease. *Biochemical Journal*, *482*(10), 603–620. https://doi.org/10.1042/BCJ20240265

Patro, R., Duggal, G., Love, M. I., Irizarry, R. A., & Kingsford, C. (2017). Salmon provides fast and bias-aware quantification of transcript expression. *Nature Methods*, *14*(4), 417–419. https://doi.org/10.1038/nmeth.4197

Pauly, M., Krumbiegel, M., Trumpp, S., Braig, S., Rupprecht, T., Kraus, C., Uebe, S., Reis, A., & Vasileiou, G. (2024). Severe manifestation of Rauch-Azzarello syndrome associated with biallelic deletion of CTNND2. *Clinical Genetics*, *106*(2), 180–186. https://doi.org/10.1111/cge.14532

Richards, S., Aziz, N., Bale, S., Bick, D., Das, S., Gastier-Foster, J., Grody, W. W., Hegde, M., Lyon, E., Spector, E., Voelkerding, K., & Rehm, H. L. (2015). Standards and guidelines for the interpretation of sequence variants: A joint consensus recommendation of the American College of Medical Genetics and Genomics and the Association for Molecular Pathology. *Genetics in Medicine*, *17*(5). https://doi.org/10.1038/gim.2015.30

Ryu, T., Park, H. J., Kim, H., Cho, Y. C., Kim, B. C., Jo, J., Seo, Y. W., Choi, W. S., & Kim, K. (2019). Improved memory and reduced anxiety in δ-catenin transgenic mice. *Experimental Neurology*, *318*, 22–31. https://doi.org/10.1016/j.expneurol.2019.04.006

Sanders, S. J., Ercan-Sencicek, A. G., Hus, V., Luo, R., Murtha, M. T., Moreno-De-Luca, D., Chu, S. H., Moreau, M. P., Gupta, A. R., Thomson, S. A., Mason, C. E., Bilguvar, K.,

Celestino-Soper, P. B. S., Choi, M., Crawford, E. L., Davis, L., Davis Wright, N. R., Dhodapkar, R. M., DiCola, M., … State, M. W. (2011). Multiple Recurrent De Novo CNVs, Including Duplications of the 7q11.23 Williams Syndrome Region, Are Strongly Associated with Autism. *Neuron*, *70*(5). https://doi.org/10.1016/j.neuron.2011.05.002

Sebastian, R., Jin, K., Pavon, N., Bansal, R., Potter, A., Song, Y., Babu, J., Gabriel, R., Sun, Y., Aronow, B., & Pak, C. H. (2023). Schizophrenia-associated NRXN1 deletions induce developmental-timing- and cell-type-specific vulnerabilities in human brain organoids. *Nature Communications*, *14*(1). https://doi.org/10.1038/s41467-023-39420-6

Sobreira, N., Schiettecatte, F., Valle, D., & Hamosh, A. (2015). GeneMatcher: A Matching Tool for Connecting Investigators with an Interest in the Same Gene. *Human Mutation*, *36*(10). https://doi.org/10.1002/humu.22844

Sudnawa, K. K., Garber, A., Cohen, R., Calamia, S., Kanner, C. H., Montes, J., Bain, J. M., Fee, R. J., & Chung, W. K. (2024). Clinical phenotypic spectrum of CTNNB1 neurodevelopmental disorder. *Clinical Genetics*, *105*(5). https://doi.org/10.1111/cge.14487

Szklarczyk, D., Kirsch, R., Koutrouli, M., Nastou, K., Mehryary, F., Hachilif, R., Gable, A. L., Fang, T., Doncheva, N. T., Pyysalo, S., Bork, P., Jensen, L. J., & Von Mering, C. (2023). The STRING database in 2023: protein-protein association networks and functional enrichment analyses for any sequenced genome of interest. *Nucleic Acids Research*, *51*(1 D), D638–D646. https://doi.org/10.1093/nar/gkac1000

Turner, T. N., Sharma, K., Oh, E. C., Liu, Y. P., Collins, R. L., Sosa, M. X., Auer, D. R., Brand, H., Sanders, S. J., Moreno-De-Luca, D., Pihur, V., Plona, T., Pike, K., Soppet, D. R., Smith, M. W., Cheung, S. W., Martin, C. L., State, M. W., Talkowski, M. E., … Chakravarti, A. (2015). Loss of δ-catenin function in severe autism. *Nature*, *520*(7545), 51–56. https://doi.org/10.1038/nature14186

Vaz, R., Edwards, S., Dueñas-Rey, A., Hofmeister, W., & Lindstrand, A. (2023). Loss of ctnnd2b affects neuronal differentiation and behavior in zebrafish. *Frontiers in Neuroscience*, *17*. https://doi.org/10.3389/fnins.2023.1205653

Wang, Y., Zhai, Y., Zhang, M., Song, C., Zhang, Y., & Zhang, G. (2024). Escaping from CRISPR-Cas-mediated knockout: the facts, mechanisms, and applications. *Cellular & Molecular Biology Letters*, *29*(1), 48. https://doi.org/10.1186/s11658-024-00565-x

Zhang, Y., Xie, K., & Jiang, T. (2025). Roles and regulation of δ-catenin in tumorigenesis and neuronal diseases. *Frontiers in Cell and Developmental Biology*, *13*, 1559059. https://doi.org/10.3389/FCELL.2025.1559059

Supplementary Files

This is a list of supplementary files associated with this preprint. Click to download.

- AdditionalFile2Supplementarymethods.docx
- AdditionalFile1TablesS114.xlsx
- AdditionalFile3FigS15.docx